

# **The Identification of Proteins Interacting with the 53BP1 Tandem Tudor Domains**

By

Kai-wei Chang

Faculty of Medicine  
Division of Experimental Medicine  
McGill University, Montreal, Quebec, Canada  
August, 2008

A Thesis Submitted to The Faculty of Graduate Studies and Research in Partial  
Fulfillment of the Requirements for the Degree of Master in Science.

© Kai-wei Chang, 2008

## Abstract

Tumor protein p53 binding protein 1 (53BP1) is a cell cycle checkpoint protein that is important in the early DNA double strand break (DSB) response signal pathway. Aberrant reduction or lack of 53BP1 is found in significant proportions of carcinomas. 53BP1 is recruited to DSB sites and forms foci through its tandem Tudor domain by recognizing dimethylated lysines in histones. The 53BP1 tandem Tudor (53BP1<sup>TT</sup>) domain consists of two tightly packed Tudor domains followed by a C-terminal alpha helix, and actively binds to methylated histone lysines H4K20 and H3K79. I hypothesized that 53BP1<sup>TT</sup> domain can potentially interact with non-histone targets, which contain methylated residues, and may be involved in the maintenance of genomic stability. The primary goal of the work presented in this thesis is to identify the proteins that interact with the 53BP1<sup>TT</sup> domain. I performed a proteomic screen by employing *in vitro* transcription/translation coupled reactions on pools of cDNA plasmids and identified two putative 53BP1<sup>TT</sup> targets, brahma-related gene 1 (BRG1), which is a chromatin remodeling catalytic subunit that has helicase and ATPase activities, and is thought to regulate transcription by altering the chromatin structure, and checkpoint kinase 1 (CHK1), which mediates DNA damage signal to downstream damage responsive proteins and initiates cell cycle checkpoint arrest. I demonstrated that both endogenous BRG1 and CHK1 interacted with the 53BP1<sup>TT</sup> domain in glutathione-S-transferase pulldown assays. Co-immunoprecipitation between ectopically expressed BRG1 and 53BP1 was observed. Interestingly, the interaction between endogenous BRG1 and 53BP1 was observed only after DNA

damage. I mapped BRG1 dimethylated lysine K1375 as the site of interaction of the 53BP1<sup>TT</sup> domain. Using a BRG1K1375me2-specific antibody, I further detected BRG1 methylation at K1375 in HeLa cells. The detected methylation signal increased in response to DNA damage. By applying cross species sequence alignment on BRG1, the BRG1K1375 was found to be conserved throughout eukaryotes. Based on this finding, the K1375 containing domain was determined to be a putative 53BP1<sup>TT</sup> domain binding motif. The observation of the interaction between 53BP1 and BRG1 provides a potential link between DNA damage response and chromatin remodeling.

## Sommaire

La protéine 53BP1 (p53 binding protein 1) (53BP1) est une protéine impliquée dans la surveillance du cycle cellulaire (checkpoint) activé par les brisures d'ADN double-brin (double-strand break ou DSB). L'absence ou la réduction d'expression de 53BP1 est une caractéristique retrouvée dans la majorité de carcinomes. 53BP1 est recrutée rapidement aux sites de DSB par ses domaines Tudor tandem qui reconnaissent les résidus de lysines diméthylées des histones. Les domaines 53BP1 Tudor tandem (53BP1TT) est comprennent deux domaines Tudor suivi par une hélice alpha au C-terminal et ces domaines ont une affinité spécifique pour les lysines méthylées H4K20 et H3K79 des histones. Étant donné que les domaines Tudor tandem sont généralement caractérisés par leur interaction avec les résidus méthylés, j'ai émis l'hypothèse que les 53BP1TT pourraient d'interagir avec des protéines autres que les histones contenant des résidus méthylés, ce qui révélerait un rôle important dans le maintien de la stabilité génomique. Donc, le principal objectif du travail présenté dans cette thèse est l'identification de protéines interagissant avec 53BP1TT. Pour ce faire, j'ai employé la réaction couplée de transcription et traduction *in vitro* sur une banque d'ADNc. Ceci m'a permis d'identifier deux cibles putatives de 53BP1TT, soit CHK1 (checkpoint kinase 1) et BRG1 (brahma-related gene 1). Chk1 est connu de jouer un rôle clé dans la cascade de signalisation des brisures d'ADN double-brin et pour son interaction avec les homologues de levure de 53BP1, tandis que BRG1 est la sous-unité ATPase des complexes SWI/SNF impliqués dans le remodelage de la chromatine. J'ai démontré par les essais pulldown avec

glutathione-S-transferase que BRG1 endogène ainsi que CHK1 endogène interagissent avec 53BP1TT. Ce travail donc établi le premier lien entre Chk1 et 53BP1 dans les cellules de mammifères. J'ai également identifié une interaction entre BRG1 et 53BP1 par co-immunoprecipitation et démontré que cette interaction est modulée par la méthylation, ainsi que par les brisures d'ADN double-brin. Cette interaction suggère un nouveau mécanisme de réponse au dommage à l'ADN, et fournit un lien entre la réponse aux dommages de l'ADN et du remodelage de la chromatine.

## Preface

This master thesis was written in the non-manuscript format in accordance with the Guidelines for Thesis Preparation provided by McGill University. I conducted all experiments presented in this thesis unless indicated otherwise. In addition, everyone who contributed to my research is acknowledged in the next section and throughout the text.

## Acknowledgements

I would like to thank my supervisor, Dr. Stéphane Richard, for giving me the opportunity to pursue my studies and research career in his laboratory and for guiding me throughout the study period.

I want to thank all lab members, whom I have met since I joined the team, for their friendly support and the great learning experience. I am grateful to Patrick Cléroux, my first mentor in the laboratory, for helping to familiarize me with the laboratory environment. Also, I thank Mélanie Morel for initiating the screening process that enabled a positive outcome of my experiments.

I want to express my gratitude to Dr. Kiven Ériq Lukong who greatly helped me with the research strategy, troubleshooting techniques, and tips for better performance. I thank Ali Salim for the assistance and collaboration on certain aspects of my project. I would also thank Drs. Yunling Wang, Zhenbao Yu, Jonathan Michaud-Levesque and Frédérick Mallette for excellent advice and stimulating discussions related to my project.

Last but not least, I am grateful for the support of my family and my fiancée, Lily Jin, who I consider a life-time partner in my science career.

This work was funded by the National Cancer Institute of Canada (NCIC) and the Cancer Research Society.

## Table of Contents

<b>ABSTRACT</b> .....	<b>II</b>
<b>SOMMAIRE</b> .....	<b>IV</b>
<b>PREFACE</b> .....	<b>VI</b>
<b>ACKNOWLEDGEMENTS</b> .....	<b>VII</b>
<b>TABLE OF CONTENTS</b> .....	<b>VIII</b>
<b>LIST OF ABBREVIATIONS</b> .....	<b>XI</b>
<b>HYPOTHESIS AND OBJECTIVE</b> .....	<b>17</b>
<b>INTRODUCTION</b> .....	<b>18</b>
<b>Genome stability – DNA damage signaling and repair</b> .....	<b>18</b>
<i>Epigenetic histone post-translational modifications guides DSB responses</i> .....	<b>20</b>
<i>Cell cycle checkpoints</i> .....	<b>20</b>
<i>DSB repair</i> .....	<b>22</b>
<b>p53 binding protein 1 (53BP1)</b> .....	<b>24</b>
<i>53BP1 and its functional domains and motifs</i> .....	<b>24</b>
<i>Phosphorylation of 53BP1</i> .....	<b>25</b>
<i>DNA binding function of 53BP1</i> .....	<b>26</b>
<i>The role of 53BP1 in DSB response</i> .....	<b>27</b>
<b>Tudor domains</b> .....	<b>29</b>
<i>Tudor domain structure</i> .....	<b>29</b>
<i>Function of Tudor domains</i> .....	<b>31</b>
<i>53BP1 tandem Tudor domain</i> .....	<b>32</b>

<b>RESULTS.....</b>	<b>42</b>
<b>cDNA pool selection .....</b>	<b>42</b>
<b>Sequence identification .....</b>	<b>45</b>
<b>Sequence alignment .....</b>	<b>49</b>
<b>Endogenous BRG1 and CHK1 in HeLa cells interact with GST-53BP1<sup>TT</sup></b>	
<b>domain.....</b>	<b>51</b>
<b>Effects of DSB on the binding affinity of 53BP1<sup>TT</sup> domain.....</b>	<b>52</b>
<b>HRK motif in BRG1 .....</b>	<b>53</b>
<b><i>In vivo</i> 53BP1-BRG1 interaction is associated to DNA damage .....</b>	<b>55</b>
<b>BRG1 can be methylated <i>in vivo</i> .....</b>	<b>57</b>
<b>BRG1K1375 methylation in response to DSBs.....</b>	<b>58</b>
<b>DISCUSSION .....</b>	<b>61</b>
<b>REFERENCES.....</b>	<b>71</b>
<b>APPENDIX.....</b>	<b>79</b>

## List of Figures and Tables

<b>Figure 1. DSB responsive pathways .....</b>	<b>19</b>
<b>Figure 2. The linear representation of 53BP1 .....</b>	<b>25</b>
<b>Figure 3. 3D structure of Tudor domains in various proteins .....</b>	<b>31</b>
<b>Figure 4. 3D image illustrating the 53BP1<sup>TT</sup> binding to H4K20me2.....</b>	<b>34</b>
<b>Figure 5. IVT products from cDNA pools obtained after sib selection.....</b>	<b>43</b>
<b>Figure 6. GST-pulldown assay using proteins from IVT .....</b>	<b>44</b>
<b>Figure 7. Probability curve of isolating a 53BP1<sup>TT</sup> binding partner.....</b>	<b>45</b>
<b>Figure 8. Matching GST-pulldown results .....</b>	<b>49</b>
<b>Figure 9. Sequence alignment of CHK1 and BRG1 protein sequences with H3K79 or H4K20 as reference sequences.....</b>	<b>51</b>
<b>Figure 10. GST-pulldown assays using total cell lysates .....</b>	<b>53</b>
<b>Figure 11. The BRG1 HRK motif and its role in 53BP1<sup>TT</sup> binding .....</b>	<b>55</b>
<b>Figure 12. <i>In vivo</i> co-immunoprecipitation of V5-BRG1 and HA-53BP1 .....</b>	<b>57</b>
<b>Figure 13. <i>In vivo</i> methylation assay .....</b>	<b>58</b>
<b>Figure 14. Anti-BRG1K1375me2 detects BRG1 HRK* motif.....</b>	<b>60</b>
<b>Figure 15. Recursive sib selection flow chart .....</b>	<b>62</b>
<b>Figure 16. Sequence alignment of 53BP1<sup>TT</sup> binding motif across species .....</b>	<b>68</b>
<b>Table 1. List of unique human genes identified from the target pools.....</b>	<b>48</b>

## List of Abbreviations

**53BP1:** p53 binding protein 1

**53BP1<sup>TT</sup>:** 53BP1 tandem Tudor

**53BP1<sup>TT</sup>BM:** 53BP1 tandem Tudor binding motif

**53BP2:** tumor protein p53 binding protein 2

**aDMA:** asymmetric dimethyl-arginine

**ATCC:** American Type Culture Collection

**ATM:** ataxia telangiectasia mutated

**ATP:** adenosine-5'-triphosphate

**ATR:** ataxia telangiectasia and Rad3 related

**BLAST:** Basic Local Alignment Search Tool

**blastx:** BLAST search protein databases using a translated nucleotide query

**bps:** base pairs

**BRCA1:** breast cancer 1

**BRCA2:** breast cancer 2

**BRCT:** BRCA1 C-terminus

**BRG1:** brahma-related gene 1

**BRG1:1080-1395:** BRG1 residue 1080 to 1395 truncation

**BRG1:1080-1360:** BRG1 residue 1080 to 1360 truncation

**BRG1K1375me2:** dimethylated lysine K1375 in BRG1

**CABLES2:** Cdk5 and Abl enzyme substrate 2

**CADOR:** chromatin-associated domain array

**CDC25:** cell division cycle 25

**CDC25A:** CDC25 homolog A

**CDK:** cyclin-dependent kinases

**cDNA:** complementary DNA

**CHEK1:** Homo sapiens CHK1 checkpoint homolog (S. pombe)

**CHK1:** checkpoint kinase 1

**CHK2:** checkpoint kinase 2

**Chromo:** chromatin-binding domain

**co-IP:** co-immunoprecipitation

**CRB2:** crumbs homolog 2

**CSR:** class switch recombination

**DFK:** asparatic acid- phenylalanine-lysine

**DMEM:** Dulbecco's Modified Eagle's Medium

**DNA:** deoxyribonucleic acid

**DNA-PK:** DNA-dependent protein kinase

**DOT1:** histone H3 methyltransferase DOT1

**DOT1L:** DOT1-like

**DSB:** double-strand break

**ELISA:** enzyme linked immunosorbent assay

**FLAG:** FLAG® (N-DYKDDDDK-C) epitope tag peptide

**G0 phase:** quiescent state, in cell cycle context

**G1 phase:** cell cycle state between mitosis and DNA replication

**G1/S:** cell cycle state boundary between G1 phase and S phase

**G2 phase:** cell cycle state between DNA replication and mitosis

**G2/M:** cell cycle state boundary between G2 phase and M phase

**GAR:** glycine and arginine rich region

**GFP:** green fluorescent protein

**GST:** glutathione-S-transferase

**H2A:** histone H2A

**H2AV:** H2A histone family, member V

**H2AX:** H2A histone family, member X

**H2B:** histone H2B

**H3:** histone H3

**H3K4:** H3 lysine 4

**H3K79:** H3 lysine 79

**H3K79me2:** dimethylated H3K79

**H4:** histone H4

**H4H18:** H4 histidine 18

**H4K20:** H4 lysine 20

**H4K20me2:** dimethylated H4K20

**HA:** hemagglutinin (N-YPYDVPDYA-C) epitope tag peptide

**HELICc:** helicase superfamily c-terminal domain

**HR:** homologous recombination

**HRK:** histidine-arginine-lysine

**HSA:** helicase and SANT associated domain

**IgG:** immunoglobulin G

**INO80:** inositol-requiring protein 80

**IP:** immunoprecipitation

**IPTG:** isopropyl  $\beta$ -D-1-thiogalactopyranoside

**IR:** ionic radiation

**IVT:** coupled in vitro transcription/translation

**JMJD2A:** jumonji domain containing 2A

**JMJD2A<sup>TT</sup>:** JMJD2A tandem Tudor

**KBD:** kinetochore binding domain

**LB:** Luria-Bertani Media

**M phase:** mitosis state in cell cycle

**MBT:** malignant brain tumor

**MDC1:** mediator of DNA damage checkpoint 1

**MRE11:** meiotic recombination 11

**MRN:** Mre11-Rad50-Nbs1

**NCBI:** National Center for Biotechnology Information

**NDRG1:** N-myc downstream regulated gene 1

**NHEJ:** non-homologous end joining

**NMR:** nuclear magnetic resonance

**p53, TP53:** tumor suppressor protein 53

**p53K370:** tumor protein 53 lysine 370

**p53K370me2:** dimethylated tumor protein 53 lysine 370

**PBS:** phosphate buffered saline

**PCR:** polymerase chain reaction

**PDB:** Protein Data Bank

**PRMT1:** protein arginine methyltransferase 1

**PWWP:** conserved proline-tryptophan-tryptophan-proline motif

**RAD51:** recombinase Rhp51

**RCSB:** Research Collaboratory for Structural Bioinformatics

**RHRK:** arginine-histidine-arginine-lysine

**RIDDLE:** radiosensitivity, immunodeficiency, dysmorphic features and learning difficulties

**RNA:** ribonucleic acid

**RPA:** replication protein A

**S phase:** DNA synthesis state in cell cycle

**SANT:** switching-defective protein 3, adaptor 2, nuclear receptor co-repressor, transcription factor

**S/TQ:** serine or threonine followed by glutamine site

**SAM68:** Src-associated in mitosis 68 kDa protein

**sDMA:** symmetric dimethyl-arginine

**SDS:** sodium dodecyl sulfate

**SDS-PAGE:** SDS- polyacrylamide gel electrophoresis

**SET8:** SET domain-containing protein 8

**shRNA:** short hairpin RNA

**SMARCA4:** SWI/SNF related, matrix associated, actin dependent regulator of chromatin, subfamily a, member 4

**SMN:** survival of motor neuron protein

**ssDNA:** single-stranded DNA

**Suv4-20h1/h2:** suppressor of variegation 4-20 homolog 1/homolog 2

**SWI/SNF:** switch/sucrose nonfermentable

**TT:** tandem Tudor

**UTR:** untranslated region

**V(D)J:** contiguous region of V, D, and J gene segments

**V5:** V5 (N-GKIPNPLLGLDST-C) tag epitope peptide

**XRCC4:** X-ray repair complementing defective repair in Chinese hamster cells 4

**YT:** yeast extract/tryptone media

**$\gamma$ H2AX:** phosphorylated H2AX

## Hypothesis and Objective

53BP1 is a key component involved in the early phase of the DNA damage response. It is recruited to the double strand DNA breaks (DSB) by recognizing the methylated lysine residues on target proteins via its tandem Tudor (53BP1<sup>TT</sup>) domain. The Tudor domain in general is known to recognize methylated residues, either lysine or arginine. I hypothesized that 53BP1<sup>TT</sup> domain can interact with the methylated residues in proteins other than histones and modulate key cellular processes including the DNA damage response. Accordingly, my objective was to identify proteins that interact with 53BP1<sup>TT</sup> domain and to determine the biological relevance of these interactions. Toward this aim, I initiated a proteomic screen for 53BP1<sup>TT</sup> domain binding partners, which led to the identification of the CHK1 kinase, as well as BRG1, that is, a component of the chromatin remodeling complex.

# Introduction

## Genome stability – DNA damage signaling and repair

DNA damage is detrimental to cell survival. It impairs normal cell functions including transcription, translation, DNA replication, and inter- and intra-molecular communications. As a result, cells that sustain high levels of DNA damage may be programmed to undergo senescence and apoptosis. There are many types of DNA damage, such as alkylated bases, cyclobutane pyrimidine dimers, replication errors, and DNA strand breaks (DSB) (Jiricny 1998; Vink et al. 2001; Neels et al. 2007; Kobayashi et al. 2008). DSB is particularly hazardous because it causes chromatin segment re-localization and leads to genome rearrangements. DNA damage can be induced metabolically through normal cell activities, such as oxidation (Cadet et al. 2003), or environmentally by stress factors, such as ionizing radiation (IR) and chemotoxins (Hanawalt et al. 2008). Because DNA damage can be commonly induced and is detrimental to cell survival, in order to maintain genome stability, eukaryotic cells are programmed with multiple defense pathways to reduce the effect of DNA damage including cell cycle checkpoints, DNA repair, protein trafficking and degradation, and genome-wide transcriptional responses (Fry et al. 2005; O'Driscoll et al. 2006). Initiation of cell cycle checkpoint control and DNA repair in response to DSB signals is illustrated in Fig. 1.

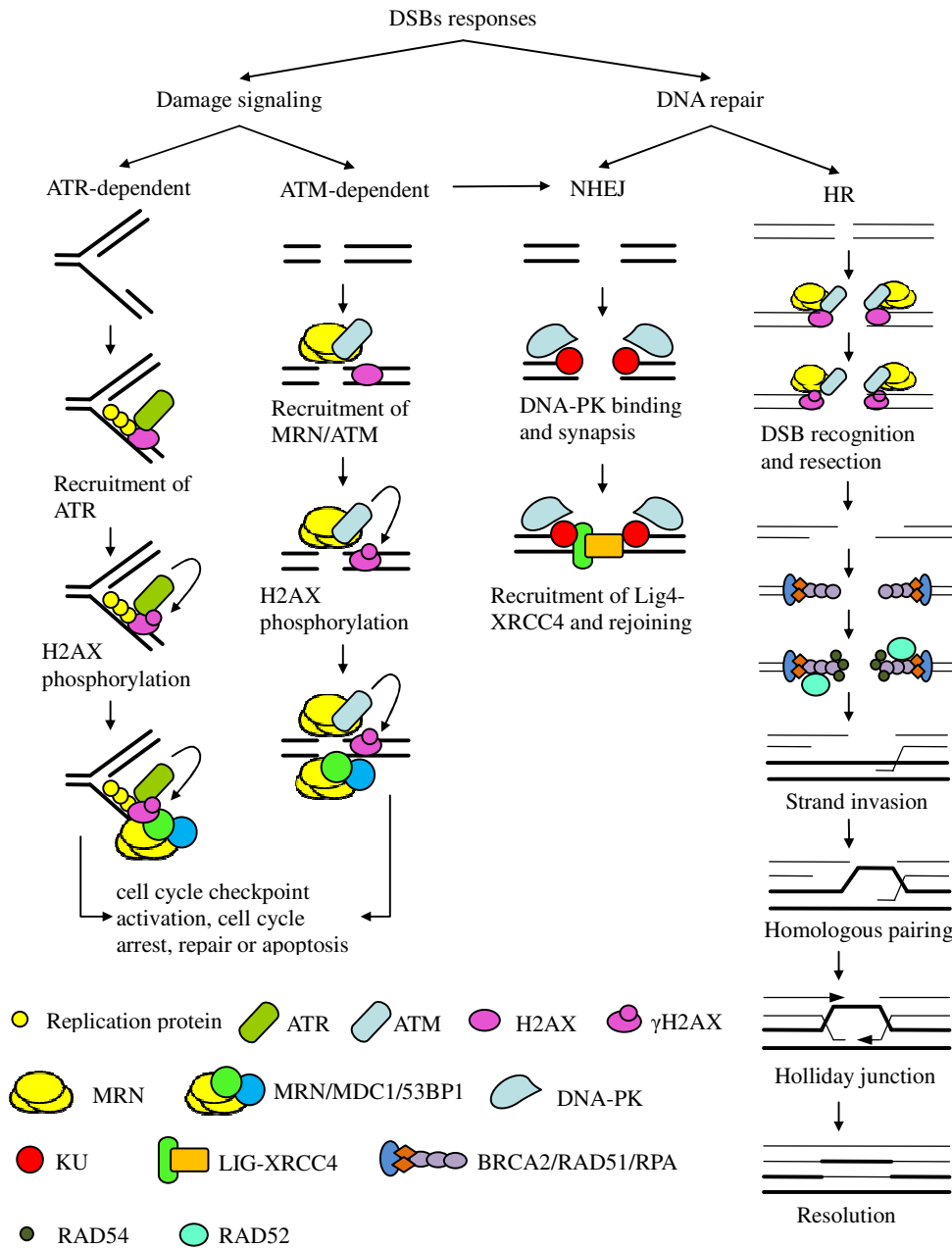


**Figure 1. DSB responsive pathways**

In response to DSB, cells activate cell cycle checkpoints and DNA repair. The cell cycle checkpoints are dependent upon either ataxia telangiectasia mutated (ATM) or ataxia telangiectasia and RAD3-related (ATR). Early damage signaling elements are listed. DSBs are repaired by either non-homologous end joining (NHEJ) or homologous recombination (HR) (Fry et al. 2005; O'Driscoll et al. 2006).

### ***Epigenetic histone post-translational modifications guides DSB responses***

Histones are basic building units for packing eukaryotic DNA into chromatin. Two of each of the core histones, H2A, H2B, H3 and H4, assemble to form one octameric nucleosome core particle by wrapping around DNA (Luger et al. 1997). Because they are wrapped around DNA and, therefore, controls cellular access to DNA, histones are modulated in cellular processes such as transcription, DNA repair, and apoptosis (Vidanes et al. 2005). Their regulation can be achieved post translationally through acetylation, ubiquitination, phosphorylation, and methylation in their tail regions (Altaf et al. 2007). These modifications were observed on all four core histones and two H2A variants, H2A member X (H2AX) and H2A member V (H2AV), in response to DSBs (van Attikum et al. 2005). Among these, phosphorylation of S139 in H2AX ( $\gamma$ H2AX) was one of the earliest responses to DNA damage and this modification promotes effective repair through multiple pathways (Vidanes et al. 2005). Moreover, lysine methylation is induced in histone tails in response to DSB and mediates the recruitment of damage responsive proteins to the DSB site (Shi et al. 2007).

### ***Cell cycle checkpoints***

Cell cycle checkpoint proteins are activated in response to DNA damage to induce cell cycle arrest, which permits the activation of DNA repair pathways before mitosis proceeds. The cell cycle consists of mitosis (M phase), followed by the G1 phase, in which the cells exhibit normal biosynthetic activities, the G0 phase, which non-proliferative cells enter from G1 phase and may proceed to S

phase under specific circumstances (ref), the S phase, which succeeds G1 or G0 phase and is characterized by chromosome replication, and the G2 phase, in which chromosome replication is completed and microtubules required for M phase are synthesized. The G2 phase precedes the M phase, completing the cell cycle (ref; review). It should be noted that transcription and translation rates slow down during S phase, with the exception of histone synthesis (Wu et al. 1981).

The DNA damage checkpoints occur at G1/S and G2/M boundaries and intra-S-phase (Bakkenist et al. 2003). The activated G1/S checkpoint signaling prevents the replication of damaged DNA; while the activated G2/M checkpoint signaling prevents the segregation of damaged chromosome during mitosis (Ishikawa et al. 2006). The intra-S-phase checkpoint, when activated, inhibits replicative DNA synthesis in presence of DNA damage (Shimada et al. 2006). The checkpoint signals are induced by ataxia telangiectasia mutated (ATM) and ataxia telangiectasia and RAD3-related (ATR) (Ishikawa et al. 2006), both are serine/threonine-specific protein kinases that regulate the activation of the DNA damage response by phosphorylation (Kurz et al. 2004). ATM responds to DSBs and disruptions in chromatin structure (Bakkenist et al. 2003), while ATR primarily responds to single-stranded DNA (ssDNA) breaks normally occur at stalled replication forks or during the repair of bulky lesions (Costanzo et al. 2003). In response to DSBs, the primary DSB sensor, Mre11-Rad50-Nbs1 (MRN) complex, recruits ATM to the DSB site (Falck et al. 2005), which then functions with DNA-dependent protein kinase (DNA-PK) redundantly to phosphorylate

H2AX (Koike et al. 2005). The phosphorylated H2AX forms strong foci around the DNA damage site, recruits and retains other mediator proteins such as mediator of DNA damage checkpoint 1 (MDC1), breast cancer 1 (BRCA1), tumor protein p53 binding protein 1 (53BP1), and MRN complex. These proteins then initiate the cell cycle arrest (Koike et al. 2005).

The ATM dependent DSB signaling pathway primarily activates G1/S and G2/M checkpoints. The G1/S checkpoint arrests cell cycle prior to DNA replication, allowing DNA repair to take place, as a result, prevents the proliferation of cells with damaged DNA. It occurs through the activation of ATM-dependent signaling pathway, followed by p53 and checkpoint kinase 2 (CHK2) phosphorylation and activation, which lead to the inhibition of cyclin-dependent kinases (CDKs) by p21 and subsequent G1/S checkpoint arrest (Guo et al. 2008). ATM also phosphorylates and activates checkpoint 1 (CHK1), which in turn inhibits the activity of cell division cycle 25 (CDC25) and CDK. This induces a G2/M checkpoint arrest (Chen et al. 1999). The ATM- and ATR-dependent DSB signaling pathways share similar downstream phosphorylation substrates and induce checkpoint arrest in a similar fashion (Stiff et al. 2006).

### ***DSB repair***

DNA repair is crucial in maintaining genome integrity. Reports indicate a tight relationship between damage signaling and DNA repair pathways (Khanna et al. 2001; Goodarzi et al. 2008). The main DNA repair pathways for DSBs

include non-homologous end joining (NHEJ) and homologous recombination (HR). Both NHEJ and HR are regulated in an ATM- and ATR- dependent manner (Kuhne et al. 2003; Matsuoka et al. 2007). NHEJ ligates the DNA ends without the requirement of sequence homologies between the two interacting molecules (Saintigny et al. 2007). This mechanism also plays a crucial role in V(D)J recombination in the immune system (Lieber et al. 2006; Soulas-Sprauel et al. 2007). The NHEJ process is initiated by the localization of a heterodimer of KU protein and DNA-PK to the DSB site (Soulas-Sprauel et al. 2007). The assembled DNA-PK complex recruits X-ray repair complementing defective repair in Chinese hamster cells 4 (XRCC4) and DNA ligase 4 to carry out the ligation (Saintigny et al. 2007). There is proficient evidence demonstrating that the function of XRCC4 in NHEJ is dependent on 53BP1 activity (Xie et al. 2007).

Opposite to NHEJ, HR requires a sister homologue template, which is generated as the result of replication-fork stalling at DSBs. HR involves a number of DSB stress response proteins, including ATM, ATR, DNA-PKs and  $\gamma$ H2AX, and a large number of downstream proteins, including recombinase Rhp51 (RAD51), RAD52, RAD54, BRCA1, BRCA2, and MRN complex (Valerie et al. 2003; Sonoda et al. 2007). HR is initiated by the invasion of single-stranded DNA into the template strand promoted by RAD51, which is recruited by BRCA2 and RAD52-replication protein A (RPA)-ssDNA nucleoprotein co-complex (Henning et al. 2003; Thorslund et al. 2007). The homologous pairing during strand invasion induces a double cross-over linking homologous DNA duplexes, called a

Holliday junction. This structure allows DNA synthesis to take place by using the sister strand as a template (Liu et al. 2004).

## **p53 binding protein 1 (53BP1)**

### *53BP1 and its functional domains and motifs*

Genomic instability, which causes the disruption of normal cell function and the loss of cell growth control, is the hallmark of most cancers. In response to DNA damage, cells attempt to suppress the disruptions and to restore the normal cell function (Aravind et al. 1999). The tumor suppressor protein 53 (TP53, also known as p53) is a key component in cancer development because mutations of P53 are associated with multiple types of cancer (Harris 1990; Unger et al. 1992). P53 functions both as a transcription factor that is induced by cellular stress factors and is a regulator of other cellular processes such as cell cycle control, cell division, and apoptosis (Oren 2003). Great attention has been given to p53-associated proteins to better understand the mechanistic roles of p53, especially in cell repair pathways. One of these proteins is 53BP1.

53BP1, maps to chromosome 15q15-21 (Iwabuchi et al. 1998) and was identified as a key component in the early responses of DNA damage. Both 53BP1 and 53BP2 were first characterized as p53-binding proteins by yeast two-hybrid screen (Iwabuchi et al. 1994). The study determined that 53BP1 binds to the central domain of p53. However, mutant p53 failed to bind to 53BP1

suggesting that 53BP1 may be involved in some aspect of p53-mediated tumor suppression (Iwabuchi et al. 1994). 53BP1 has four functional regions: various phosphorylation sites (S/TQ), two tandem BRCA1 C-terminus (BRCT) domains, a glycine-arginine rich (GAR) motif, and two tandem Tudor (53BP1<sup>TT</sup>) domains (Fig. 2). The 53BP1 tandem BRCT domain identified as p53 binding site is homologous to the BRCA1 tandem BRCT region. This region is involved in DSB repair and homologous recombination (Joo et al. 2002). The genetically conserved first BRCT repeat and the inter-BRCT linker of 53BP1 have been shown to bind to p53 in a region that overlaps with the DNA-binding surface of p53 (Derbyshire et al. 2002). The interaction between 53BP1 and p53 is reported to enhance p53-mediated transcriptional activation (Iwabuchi et al. 1998).



**Figure 2. The linear representation of 53BP1**

Human 53BP1 contains 1972 amino acids with four functional regions as indicated. The S/TQ site is phosphorylated after binding to DNA. GAR motif contains arginines that can be methylated by protein arginine methyltransferase 1 (PRMT1). Tandem Tudor domains recognize dimethylated H3K79 and H4K20. Tandem BRCTs bind to p53 and are associated to p53 mediated damage response pathways.

### ***Phosphorylation of 53BP1***

Experiments focused on DNA damage-signaling pathways revealed that 53BP1 becomes hyper-phosphorylated and forms discrete nuclear foci at sites of

DNA damage (Rappold et al. 2001; Huyen et al. 2004). Additionally, 53BP1 was determined to be an *in vitro* and *in vivo* phosphorylation substrate of ATM (Xia et al. 2001). There is evidence that the absence or inhibition of ATM-related kinase delays the re-localization and phosphorylation of 53BP1 in response to ionizing radiation induced DNA damage (Anderson et al. 2001). This suggests that 53BP1 participates in an ATM phosphorylation-dependent checkpoint control and DNA repair. 53BP1 co-localizes with other DSB response factors such as H2AX at DSB sites (Ward et al. 2003). Interestingly, the recruitment of 53BP1 to DSB sites appears to be independent of other proteins (Mochan et al. 2004), which implies that the former is an upstream element that interacts with DNA in response to DSBs. Furthermore, immunofluorescence staining of cells ectopically expressing 53BP1 deletion mutants determined that the minimal domain for foci formation is composed of the conserved Tudor domain and Myb motif (Iwabuchi et al. 2003), both of which in combination were later defined as the 53BP1 tandem Tudor domain.

### ***DNA binding function of 53BP1***

During mitosis, endogenous 53BP1, as well as ectopically expressed green fluorescent protein (GFP)-tagged 53BP1, were found localized to the kinetochores (Jullien et al. 2002). The 53BP1 kinetochore binding domain (KBD) was mapped to 380 residues upstream of the 53BP1 BRCT domain (Jullien et al. 2002). The 53BP1 KBD contains a GAR motif (Boisvert et al. 2005) and the tandem Tudor domain (Iwabuchi et al. 2003). Arginines in the 53BP1 GAR motif are

asymmetrically dimethylated by protein arginine methyltransferase 1 (PRMT1) (Boisvert et al. 2005). PRMT1 also methylates meiotic recombination 11 (MRE11), which is a component of the MRN complex involved in DNA repair in mammalian cells (Jazayeri et al. 2008). Amino acid substitution of the arginines within the 53BP1 GAR motif abrogates DNA binding, demonstrating the importance of GAR motif in mediating DNA binding activity (Boisvert et al. 2005). Hence, the 53BP1 GAR motif plays a role in DNA binding and 53BP1 localization to chromatin.

#### ***The role of 53BP1 in DSB response***

53BP1 contributes in mediating both the checkpoint arrest and DNA repair pathways during DSB response (Schultz et al. 2000). The direct interaction of 53BP1 to DNA on DSB sites implies a DSB sensing role of 53BP1 (DiTullio et al. 2002; Celeste et al. 2003). The re-localization of 53BP1 to DSB sites mediates and promotes the activation of ATM, which subsequently phosphorylates p53, 53BP1,  $\gamma$ H2AX and other signaling mediators (Mochan et al. 2004; Jowsey et al. 2007). In addition, the association between 53BP1 and p53 further enhances the activity of 53BP1. In the telomere-initiated senescence scenario, the DSB response is triggered by telomere shortening or uncapping. This results in the co-localization of  $\gamma$ H2AX and 53BP1 and subsequent checkpoint activation (d'Adda di Fagnana et al. 2003). Although the localization of 53BP1 to the damage sites is independent of  $\gamma$ H2AX, it is required for the retention and the subsequent increase in the local concentration of 53BP1 at sites of DNA damage (Celeste et al. 2003).

53BP1 also associates with the activity of the core NHEJ element XRCC4, illustrating a direct involvement of 53BP1 in DSB repair (Xie et al. 2007).

53BP1-null cells are hypersensitive to IR and display hyper-recombination phenotype (Adams et al. 2005). A robust knockdown of 53BP1 expression with siRNA impairs the phosphorylation of two known ATM substrates, p53 and BRCA1, in IR-damaged cells (Wang et al. 2002). In addition, 53BP1- and ATM-null cells share similar phenotypes after IR (Minter-Dykhouse et al. 2008). Together, this implies that 53BP1 plays a role in checkpoint regulation. This is consistent with the phenotype in 53BP1-null mice, which is characterized by severe class switch recombination (CSR) and decreased number of mature T cells (Manis et al. 2004). 53BP1 functions in NHEJ in an XRCC4-dependent and  $\gamma$ H2AX-independent manner, but has a suppressive role in HR (Xie et al. 2007). This suggests that 53BP1 may be an important factor for cells to decide whether to repair DSBs by NHEJ or HR. Cells from patients displaying RIDDLE (radiosensitivity, immunodeficiency, dysmorphic features and learning difficulties) syndrome were found to be depleted of 53BP1. Consequently, cells from patients exhibit hypersensitivity to IR, cell cycle checkpoint abnormalities, and impaired end-joining in the recombined switch regions (Stewart et al. 2007). This phenotype provides further evidence for the association of 53BP1 with cell cycle checkpoint and DSB repair.

## **Tudor domains**

The Tudor domain was originally identified in the *Drosophila* TUDOR protein (Ponting 1997). It is composed of approximately 50 residues and is structurally conserved throughout evolution. The *Drosophila* TUDOR protein is essential for the localization of mitochondrial RNAs in polar granules in *Drosophila* embryos (Amikura et al. 2001). Sequence- and structure-dependent approaches determined that the Tudor domain is homologous with conserved proline-tryptophan-tryptophan-proline motif (PWWP), chromatin-binding (Chromo) domain and malignant brain tumor (MBT) domain, which are all members of the 'Royal domain family' (Maurer-Stroh et al. 2003). Although the function of the Tudor domains has not been fully elucidated, the domain is known to mediate protein-protein interactions. Furthermore, recent studies suggested that the Tudor domain recognizes methylated arginine and lysine residues (Cote et al. 2005; Kim et al. 2006).

### ***Tudor domain structure***

The three-dimensional structure of the Tudor domain was determined by heteronuclear multidimensional nuclear magnetic resonance (NMR) spectroscopy (Selenko et al. 2001). Its central region is a  $\beta$ -barrel that comprises of five anti-parallel  $\beta$ -strands (Fig. 3), which are stabilized by the conserved residues in its hydrophobic core (Selenko et al. 2001). The conserved aromatic residues, tryptophan and tyrosine, form a cluster of hydrophobic side chains and exhibit a hydrophobic patch that fits tightly with methylated substrates (Selenko et al.

2001; Lee et al. 2008). The identified core structure of the Tudor domain is conserved in all Tudor domain-containing proteins (Selenko et al. 2001). The Tudor domain exists in single or multiple copies in proteins (Ponting 1997; Talbot et al. 1998; Huyen et al. 2004). The survival of motor neuron protein (SMN), for example, contains a single Tudor domain while the *Drosophila* TUDOR protein contains ten. Proteins containing two consecutive Tudor domains (tandem Tudor) show typical Tudor core structures in each individual region. However, variations in the link region define the uniqueness of the Tudor structure in each protein.

The 53BP1 tandem Tudor domain consists of two consecutive Tudor structures, both of which display typical Tudor domain topology, and a C-terminus  $\alpha$ -helix bridging the two Tudor regions (Charier et al. 2004). The hydrophobic pocket for the ligand binding region in 53BP1<sup>TT</sup> resides in its first Tudor motif (Fig. 3). In contrast, histone demethylase, jumonji domain containing 2A (JMJD2A), displays a “hybrid” tandem Tudor domain (JMJD2A<sup>TT</sup>) (Huang et al. 2006). In JMJD2A<sup>TT</sup>, the two Tudor domains share the same  $\beta$ -strands in their barrel cores, hence form a bilobal, saddle-shaped structure with each lobe resembling the canonical Tudor domain structure (Huang et al. 2006) (Fig. 3). Most Tudor-containing proteins were not fully characterized. However, proteins such as 53BP1, PHF20, JMJD2A, and SMN, which bind to methylated protein residues and associate to nucleotides, imply a functional trend for Tudor-containing proteins.

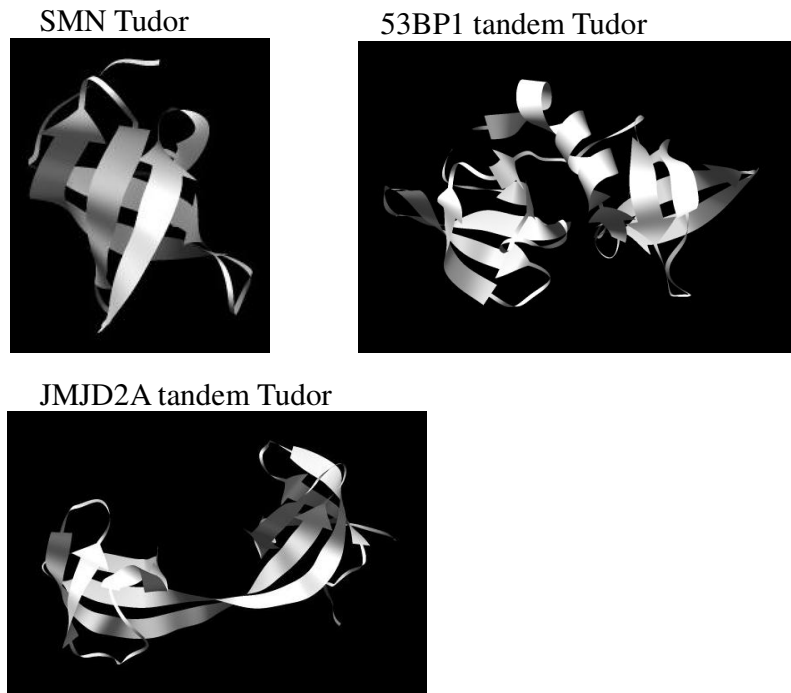


**Figure 3. 3D structure of Tudor domains in various proteins**

3D image of the Tudor domain of SMN, 53BP1 and JMJD2A. The domain structure data was obtained from Research Collaboratory for Structural Bioinformatics (RCSB) Protein Data Bank (PDB) online database (<http://www.rcsb.org>) and is visually displayed by UCSF Chimera visualization system.

### ***Function of Tudor domains***

The Tudor domain interacts with methylated protein residues. Its negatively charged electrostatic potential surface enhances the binding affinity (Selenko et al. 2001). In SMN, the Tudor domain mediates interactions with the Sm proteins. Specifically, the SMN Tudor domain binds to the symmetric and asymmetric dimethyl-arginine (sDMA and aDMA) at the GAR region in Sm

proteins (Sprangers et al. 2003; Cheng et al. 2007). This association is essential for the assembly of spliceosomal uridine-rich small nuclear ribonucleoprotein complexes (Selenko et al. 2001). The JMJD2A<sup>TT</sup>, in contrast, targets the di- and tri-methylated histone lysine H3K4 and H4K20 (Huang et al. 2006; Kim et al. 2006). The 53BP1<sup>TT</sup> interacts with dimethylated lysine on histone H3K79 and H4K20 (Huyen et al. 2004; Kim et al. 2006) and illustrates its chromatin binding function. This interaction takes place on DSB site and enhances the DSB sensing role of 53BP1.

### ***53BP1 tandem Tudor domain***

The 53BP1 tandem Tudor domain is downstream of the GAR motif in the KBD. The 53BP1 yeast homolog, crumbs homolog 2 (CRB2), displays binding affinity for H4K20 (Sanders et al. 2004; Botuyan et al. 2006). The detection of known methyl-dependent interactions using chromatin-associated domain array (CADOR) chip further validates the interaction between 53BP1<sup>TT</sup> and dimethyl-H4K20 (H4K20me<sub>2</sub>) (Kim et al. 2006). The 3D representation of 53BP1<sup>TT</sup> domain-H4K20me<sub>2</sub> interaction is illustrated in Fig. 4. 53BP1 was also found to bind to dimethylated H3K79 (H3K79me<sub>2</sub>) (Huyen et al. 2004). Intriguingly, short hairpin RNA (shRNA) knockdown of DOT1-like histone H3 methyltransferase (Dot1L) shows no effect on re-localization of 53BP1 after ionizing radiation (Botuyan et al. 2006). This implies that H3K79me<sub>2</sub> is not essential for the DSB response. Nevertheless, the discovery of the interaction between 53BP1<sup>TT</sup> and histone methyl-lysine demonstrates that 53BP1<sup>TT</sup> is required for focus formation

on DSB site. This finding also suggests that 53BP1 chromatin binding ability is associated to histone methylation (Huyen et al. 2004). Interestingly, co-immunoprecipitation using FLAG- and hemagglutinin (HA)-tagged 53BP1 determined that 53BP1 oligomerization is independent of methylated GAR motif and the function of 53BP1<sup>TT</sup> (Adams et al. 2005). The disruption of 53BP1<sup>TT</sup> by inactivating point mutation not only abolishes laser-generated DSB tracks, but also accelerates the 53BP1 mobility in undamaged cells (Bekker-Jensen et al. 2005). Taken together, the integrity of 53BP1<sup>TT</sup> affects both the DSB surveillance function of 53BP1 and its physiological chromatin binding rate (Bekker-Jensen et al. 2005).

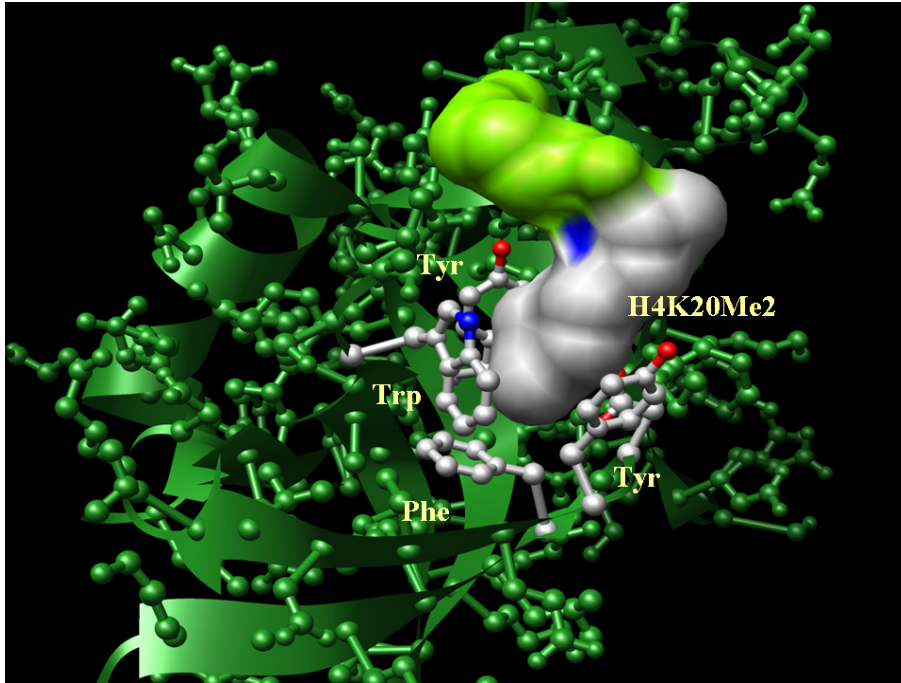


**Figure 4. 3D image illustrating the 53BP1<sup>TT</sup> binding to H4K20me2**

The hydrophobic pocket of 53BP1<sup>TT</sup> is formed by aromatic residues as labeled. The surface of H4K20me2 is hydrophobic that fits the binding site as displayed. The domain structure data was obtained from RCSB PDB online database and is visually displayed by UCSF Chimera visualization system.

To identify the 53BP1<sup>TT</sup> domain non-histone targets, I performed a proteomic screen by employing *in vitro* transcription/translation coupled reactions on pools of cDNA plasmids and identified two novel 53BP1<sup>TT</sup> targets, brahma-related gene 1 (BRG1) and checkpoint kinase 1 (CHK1). I further determined that 53BP1 and BRG1 interact in response to DNA damage in a methylation-dependent manner. The following sections will describe the identification of the proteins that interact with 53BP1 at its tandem Tudor domain in the context of DSB and methylation signal pathways.

## Materials and Methods

### *DNA constructs:*

All DNA constructs used in this work were previously generated and donated from other laboratories. Fusion protein constructs, HA-53BP1 and GST-53BP1<sup>TT</sup>, were kindly provided by Dr. Aidan J. Doherty (Boisvert et al. 2005) and the generating procedures have been described (Iwabuchi et al. 2003). V5-BRG1 was a kind gift from Dr. Trevor K. Archer (Trotter et al. 2008). HA-BRG1 plasmid and BRG1:1080-1395 plasmid were kindly provided by Dr. Paola A. Marignani (Marignani et al. 2001). The insert in the BRG1:1080-1395 vector was amplified using the T7 promoter primer, 5'-TAA TAC GAC TCA CTA TAG GG-3', the BGH reverse primer, 5'-TAG AAG GCA CAG TCG AGG-3'. The linear BRG1:1080-1360 DNA segment was synthesized from the same plasmid, using T7 promoter primer and the BRG1:1080-1360 reverse primer, 5'-GCC GAA TTC TCA CTC CTC ACA GGT CAG CCG CTC-3'. GE Healthcare illustra<sup>TM</sup> Taq DNA polymerase kit was applied using manufacture's protocol for the polymerase chain reaction (PCR).

### *Peptides:*

All peptides were synthesized by Keck Centre (Yale University, New Haven, CT). The biotinylated peptides were generated with or without methyl-modified residues. Peptides mapping 53BP1 GAR motif are as follows: 53BP1GAR (KAPVTPRGRGRRRGRPPSRTT-biotin) and 53BP1GAR\* (KAPVTPR\*GR\*GRR\*GR\*PPSRTT-biotin, R\*-asymmetric dimethyl-arginine).

Peptides mapping the hypothesized 53BP1<sup>TT</sup> binding region (see Results) in BRG1 are as follows: BRG1HRK (BRG1HRKMFGRGSRHRKEVDYSDSLT-biotin) and BRG1HRK\* (MFGRGSRHRK\*EVDYSDSLT-biotin, K\*-dimethyl-lysine).

*cDNA libraries:*

The cDNA libraries used in the project were generated using sib selection method and were kindly provided by Dr. Paola Marignani (Dalhousie University, Nova Scotia) (Marignani et al. 2001). The cDNA fragments were inserted to Invitrogen pcDNA3.1(+) vector at the EcoRI restriction site in the polylinker region.

*Antibodies:*

The anti-53BP1 rabbit polyclonal antibody was purchased from Novus Biologicals Inc (Littleton, CO). Mouse monoclonal anti-H4K20me2 and rabbit polyclonal anti-SAM68 and anti-BRG1 antibodies were purchased from Millipore. Anti-CHK1(G4) and anti-V5 mouse monoclonal antibodies were purchased from Santa Cruz Biotechnology Inc. and Sigma-Aldrich, respectively. Anti-HA antibody from mouse ascites was generated by American Type Culture Collection (ATCC) (Manassas, VA). Affinity purified rabbit polyclonal anti-GST antibody were generated at Pocono Rabbit Farm and Laboratory Inc (Canadensis, PA). Rabbit polyclonal anti-BRG1K1375me2 antibody was generated using keyhole limpet hemagglutinin-coupled MFGRGSRHRK\*EVDYSDSLT (K\* – dimethyl

lysine). For secondary antibodies in western blot, immunoreactive proteins were visualized using goat anti-mouse and goat anti-rabbit antibodies (Cedarlane Laboratories Ltd. and Sigma-Aldrich) conjugated to Western Lightning™ Chemiluminescence Reagent Plus from PerkinElmer (Waltham, MA).

*Tissue Culture:*

The cervical cancer cell line, HeLa, and the human embryonic kidney cell line, HEK293T, obtained from ATCC were used in this project. The cells were maintained in complete Dulbecco's modified Eagle's medium (DMEM) media (HyClone), containing 10% bovine calf serum, streptomycin and penicillin, and supplemented with 1mM sodium pyruvate, and 1mM L-glutamine (Wisent). The cells were maintained in 5% CO<sub>2</sub> at 37°C. Cells were cryopreserved in media containing 70% fetal bovine serum, 15% complete-DMEM, and 15% Dimethyl sulfoxide (DMSO).

*Coupled in vitro transcription/translation (IVT):*

Promega's TnT® T7 Quick Coupled Transcription/Translation System was used as the master reagent mix to synthesize proteins of interest using plasmid DNAs or PCR products as templates *in vitro*. The IVT requires T7 promoter on the templates to initiate the transcription. EasyTag™ L-<sup>35</sup>S-methionine (PerkinElmer) was applied to radioactively label the synthesized protein per reaction. In this project, the standard reaction uses 10 µl of IVT master mix, 1 µg of DNA template, and 0.5 µl of 1mCi/ml L-<sup>35</sup>S-methionine for 90 minutes at 30°C.

*Protein purification:*

*E. coli* strains containing GST (pGEX-KG) and GST-fusion protein-expressing vectors were cultured in 100 ml of LB medium with ampicillin at 37°C overnight. The culture was then transferred into 1000 ml of 2X yeast extract/tryptone (YT) media with ampicillin and incubated for one hour. Protein expression was induced with 220µl of 0.5 M isopropyl β-D-1-thiogalactopyranoside (IPTG) for three hours. The bacteria were harvested and then were resuspended in 10 ml of phosphate buffered saline (PBS). After sonication, the insoluble fractions were removed by centrifugation. The supernatant was adjusted to 1% Triton X-100 and incubated with 500 µl of 50% glutathione-sepharose beads slurry at 4°C overnight. After three washes with PBS, the beads were then resuspended in 10 mM glutathione reduced, pH7.5, to elute bound proteins. The proteins were dialyzed with PBS to remove glutathione and stored at -80°C, or at 4°C for immediate use.

*GST-pulldown assay:*

IVT products or cell lysates were suspended in 1% Triton lysis buffer (1% Triton X-100, 150 mM NaCl, 50 mM Tris, pH8.0, and 1 µg/ml of aprotinin, optional 0.25% deoxycholate and 0.1% SDS). 10 µg of purified GST-fusion prey protein was added to each sample in 4°C environment, and 20 µl of 50% glutathione-Sepharose bead slurry was subsequently added after one hour tumbling. Alternatively, the GST-fusion prey protein was pre-bound to Affi-Gel bead before loading to the samples. The samples were washed twice with lysis

buffer and once with PBS. Protein samples were analyzed by SDS-PAGE (8% or 10% acrylamide). Based on the visualizing techniques, the samples were either dried on filter paper (for radioactively labeled proteins) or transferred to nitrocellulose membranes for western blot analysis. Western blotting was performed using the primary antibodies for the proteins of interest. Goat anti-rabbit or goat anti-mouse antibodies were used as secondary antibodies. Western Lightning™ Chemiluminescence Reagent Plus from PerkinElmer was used to visualize the immunoreactive proteins.

*Enzyme-linked immunosorbent assay (ELISA):*

The biotinylated oligopeptides, dissolved in carbonate/bicarbonate buffer (50 mM NaHCO<sub>3</sub> and 50 mM Na<sub>2</sub>CO<sub>3</sub>, pH9.6) or PBS, were loaded on streptavidin coated 96-well plate from Sigma-Aldrich overnight. For sandwich ELISA only, 1 µg of GST-53BP1<sup>TT</sup> (per sample) dissolved in primary antibody buffer (2% BSA, 2.5% NaCl, 10 mM Tris, pH 7.4, 0.5% ovalbumin) was applied. To determine the protein-protein or protein-antibody binding affinity, site-specific primary antibody (rabbit anti-GST antibody for sandwich ELISA), and goat anti-rabbit or goat anti-mouse antibodies were used. BM Blue POD substrate (Roche) was used for visualization and measurement of optic density. The absorption wavelength was set at 405 nm against the reference wavelength at 490 nm.

*Heat-shock Transformation:*

1 µl of plasmid from purified source or cDNA library was added to 50 µl

competent *E. coli* strain and incubated 30 minutes on ice. The sample was heat shocked at 42°C for 90 seconds, and then cooled on ice for five minutes. The sample was dissolved in 500 µl of LB and was incubated in a 37°C shaker for 40 minutes. The sample was plated evenly on LB-agarose plate (LB with 1.5% agarose) with appropriate antibiotics for selection and was incubated at 37°C. The transformed bacteria were harvested after incubating for 14 hours.

*Cell transfection:*

Lipofectamine 2000™ from Invitrogen was used as transfection reagent to transfect either HEK293T or HeLa cells. The transfection mix consisted of 4 µg expression vectors and 60 µl Lipofectamine 2000™ in 3 ml of DMEM. It was applied to 30% of trypsinized cells from an 80%-confluent 100 mm tissue culture dish. The transfected cells were evenly distributed to a 100 mm tissue culture dish in 15 ml of DMEM with 10% bovine calf serum and incubated overnight in 5% CO<sub>2</sub> at 37°C.

*In vivo methylation:*

Methionine free DMEM (Wisent), supplemented with 100 µg/µl of cycloheximide, and 40 µg/µl of chloramphenicol, was used to replace complete-DMEM for cells in 70% confluent 100 mm tissue culture dish. After one-hour incubation, 500 µl of 1mCi/ml [methyl-<sup>3</sup>H]-methionine (PerkinElmer) was added and incubated for three hours. The cells were harvested and analyzed subsequently.

*Acid extraction:*

Cell lysates were suspended in 1% Triton lysis buffer (composition described above). The pellets were isolated and incubated with 50  $\mu$ l of 2 N HCl for 30 minutes on ice. After acid extraction, the samples were resuspended in the lysis buffer and titrated with 2 N NaOH to adjust the pH to approximately 8. The samples were used for subsequent analysis as discussed above.

*Immunoprecipitation (IP):*

Cell lysates were resuspended in 1% Triton lysis buffer (component as described previously). After removing the pellet, the cell lysates were incubated with primary antibodies, or with mouse/rabbit immunoglobulin G (IgG) as control, at 4°C, with constant end-over-end mixing (tumbling) for one hour. Then 20  $\mu$ l of 50% protein A-Sepharose coated beads slurry was added to the cell lysates and tumbled at 4°C, for one hour. The samples were washed twice with the lysis buffer and once with PBS. Protein samples were analyzed by SDS-PAGE (8% or 10% acrylamide). Western blotting was performed and visualized as described previously.

## Results

### cDNA pool selection

To screen for 53BP1<sup>TT</sup> associated proteins, 100 pools, each estimated to contain approximately 100 unique genes at random, were used in this project (Marignani et al. 2001). Proteins labeled with <sup>35</sup>S-methionine were generated by using the Promega TNT® T7 quick coupled transcription/translation (IVT) system. The IVT products were denatured and loaded to 12% pre-cast Tris-HCl gel (Bio-RAD) for SDS-PAGE, and the <sup>35</sup>S-products were visualized by fluorography. IVT products were visible on all pools and a representation of the <sup>35</sup>S-proteins generated from 9 random cDNA pools is shown in Fig. 5. To select the pools that contain potential 53BP1<sup>TT</sup> binding partners, GST-pulldown assay using the radioactively labeled IVT products from rabbit reticulocyte lysates was applied. Proteins produced in rabbit reticulocyte lysates are known to be highly methylated and are therefore good sources of ligands for methyl-interacting domains (Cheng et al. 2007; Guccione et al. 2007). Therefore, the positive hits from the proteomic screen should represent methyl-based interaction between 53BP1<sup>TT</sup> and the IVT product. The <sup>35</sup>S-methionine labeled IVT proteins were subjected to pulldown with glutathione-S-transferase (GST) alone as control and GST-53BP1<sup>TT</sup> domain fusion protein bound to Affi-Gel beads. The proteins were resolved using SDS-PAGE on 10% acrylamide gels and visualized by fluorography. I identified five target pools, numbered 606, 615, 628, 642, and 664 which contained proteins that were bound to the 53BP1<sup>TT</sup> domain (Fig. 6).

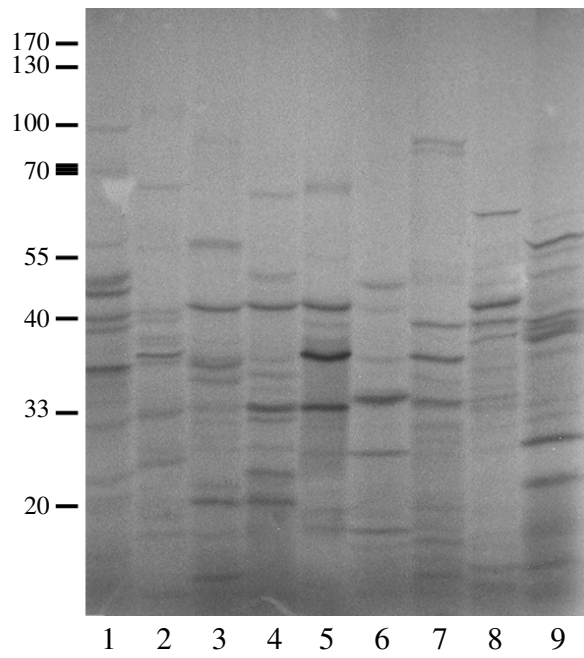


**Figure 5. IVT products from cDNA pools obtained after sib selection**

The representation of the  $^{35}\text{S}$  labeled proteins from IVT system. The proteins were separated by SDS-PAGE and visualized by fluorography.

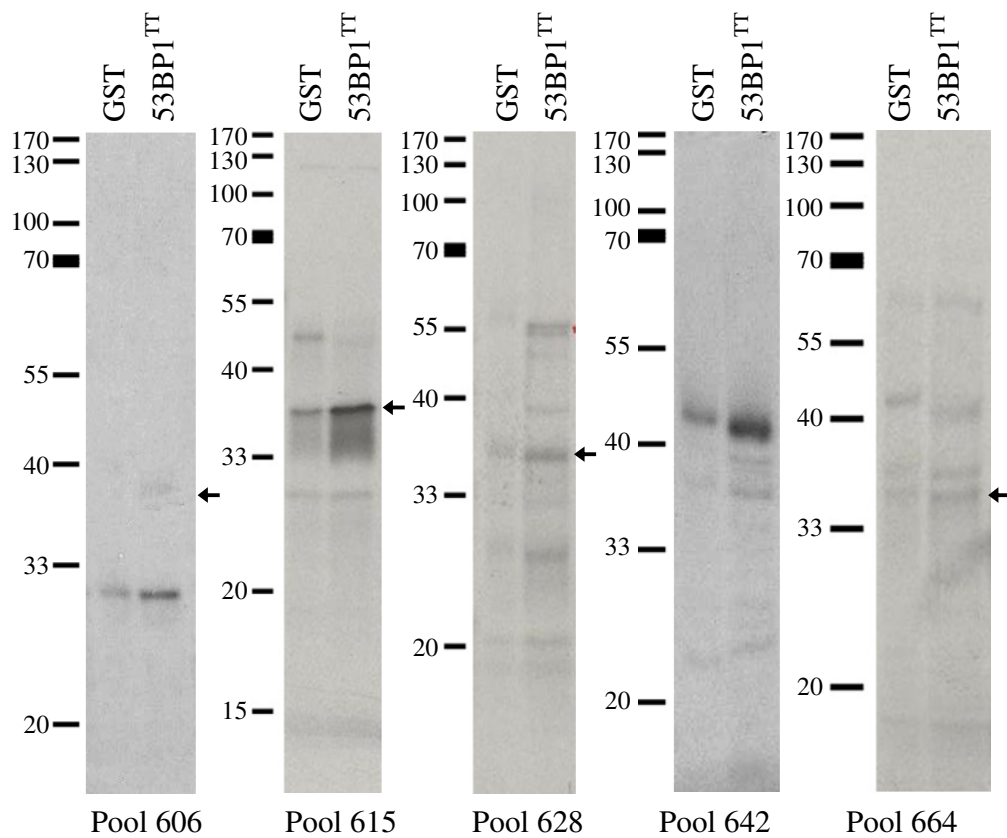


**Figure 6. GST-pulldown assay using proteins from IVT**

Radioactive  $^{35}\text{S}$ -methionine for protein labeling was used in IVT. All five pools had bands that were presented or show relatively significant binding affinity on 53BP1<sup>TT</sup> lane. These bands are at range between 33kDa and 55kDa.

## Sequence identification

In order to determine the 53BP1<sup>TT</sup> domain binding partners from the five target pools, I attempted to isolate and identify the cDNAs by transformation. A DNA aliquot of each target pool was subjected to transform competent *E. coli* strain, DH5 $\alpha$ . I assumed that each target pool contains at least one unique gene, a hit, which fits the selection criteria. I further assumed that each cDNA pool contains equal amount of unique genes and have equal chance to transform bacteria. Based on the number of unique genes in a cDNA pool and the assumptions above, the probability of finding one hit in a random transformed bacteria is at least 1%. The probability curve of isolating a hit from a number of transformants is demonstrated in Fig. 7. The actual probability, however, is above the curve since it is possible that a target pool contains more than one hit.

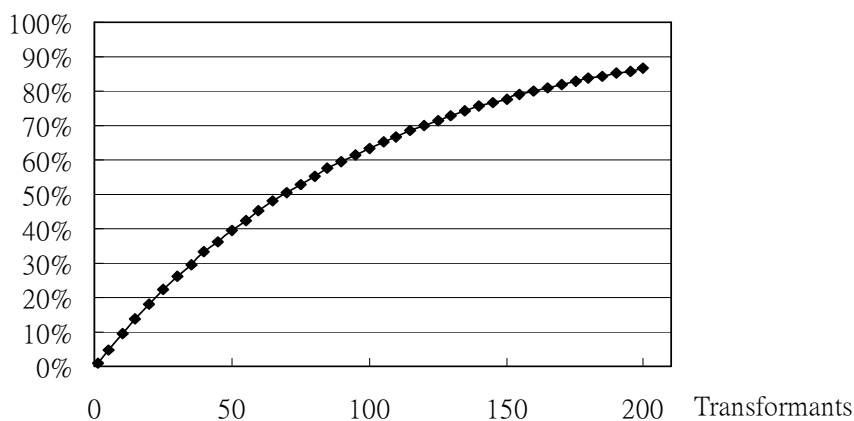


**Figure 7. Probability curve of isolating a 53BP1<sup>TT</sup> binding partner**

Let  $p = 0.01$  implying the probability of finding a hit. The probability of finding no hits is exponentially inverse proportional to the number of transformants. The probability of harvesting a hit is hence calculated.

Based on probability analysis, I hypothesized that 60% chance of finding a hit from a target pool is sufficient for identifying 53BP1<sup>TT</sup> binding partners. 100 transformed colonies were randomly selected with the assumption that each colony contains one type of amplified cDNA. The plasmids were isolated by miniprep purification. 500 miniprep samples were sent to Genome Quebec Innovation Centre (QC, Canada) for sequencing using the T7 promoter primer. Each sequence was identified by searching the National Center for Biotechnology Information (NCBI) online human gene database with Basic Local Alignment Search Tool (BLAST) online service (Altschul et al. 1990). Both search-a-protein-database (blastx) and search-a-nucleotide-database (nucleotide blast) options were used in this search. 172 colonies were determined to contain human genes, of which 148 unique genes were identified (Table 1). The 60% possibility from uniformly distributed cDNAs also implied that approximately 300 unique insert patterns will be identified. Indeed, we identified 288 unique DNA patterns from sequencing, suggesting uniform distribution of the individual inserts in the pools and comparable transformation efficiency. Radioactive labeled IVT and subsequent GST-pulldown assay were applied to all identified genes.

The mass of the generated proteins were compared to the mass of the positives observed using the pooled cDNA. Four protein candidates, one from each pool (pools 606, 615, 628, and 664) were identified to interact with 53BP1<sup>TT</sup>. I identified BRG1 (also known as SMARCA4 and SNF2), CHK1 (also known as CHEK1 in human), Cdk5 and Abl enzyme substrate 2 (CABLES2), and N-myc

downstream regulated gene 1 (NDRG1) as the candidate for pools 606, 615, 628, and 664 respectively (Fig. 8). Pool 642 may need more clones to find a hit or may represent a false-positive pool. BRG1 is the catalytic core subunit in switch/sucrose nonfermentable (SWI/SNF) related chromatin remodeling complex which regulates the accessibility of DNA (Hendricks et al. 2004). The serine-threonine kinase CHK1 is an important checkpoint kinase in DSB response pathway (Rodriguez et al. 2006). Since BRG1 and CHK1 are linked with cell cycle checkpoints and the DNA damage pathway, both proteins were especially of interest and were further characterized for their functional link to 53BP1.

**Table 1. List of unique human genes identified from the target pools**

ABCF1	CSNK2B	GPR175	M-RIP	SCN2B
ABHD11	CTSB	GTSE1	MRLC2	SDHA
ACOT7	CTSL	HADHB	MYBL2	sequence surrounding NotI site
ADAMTSL4	CUGBP1	HDLBP	antigen SHUJUN-1	SETD7
Adrenal gland protein AD-003	CXCL2	HEATR1	NDRG1	SLC2A3
AES	CYB5R1	HLA-B associated transcript 8 BAT8	NFATC2IP	SLC3A2
ALDOA	D123 gene product variant	HMG20B	NR3C1	SMARCA4 (BRG1)
ANXA2	DGCR2	HMGX2	OTUD5	SMARCD1
AP3M2	DKC1	HNRPM	PGK1	SMC4
ASCC3L1	DOM3Z	HP1-Hs-gamma pseudogene	PHB	SND1
ATP1A1	D-prohibitin	HSP90AA1	PHGDH	SOD
ATPIF1	DPYD	HSPD1	PICALM	STAU1
AURKA	E2IG3	HUMP68	PLK2	STC
B3GAT3	EEF1A1	IGFBP3	POM121	TENC1
BAIAP2	EEF1G	INPPL1	PPAP2C	tetratricopeptide repeat domain 1
BCKDK	EHMT2	IRAK2	PPP1CC	TFCP2
Beta actin variant	EIF3S1	ischemia/reperfusion inducible protein	PPP1R3B	THAP4
BNIP3	EMD	ITGB4	PQBP1	TIMP1
CABLES2	EML2	JARID1A	PRDM1	TM4SF1
CAPN1	ENO1	JTB	PRKAG1	TMEM14B
CD55	EPRS	K-ALPHA-1	PRP4K	TSGP-L Mtna
CHEK1 (CHK1)	ERP29	KIAA1429	Pscd1	TUBB
CIZ1	FASN	KIAA1949	PSMB7	UBE2T
CLG1	FGD6	KIP gene	PSMB8	VAMP2
CMAS	FOLR1	KRT17	PSMD2	WDR45
COPS3	FRG1	LARP5	PSRC1	XPNPEP1
COX4I1	FTH1	LGALS1	QARS	YTHDF1
COX7A2L	GAL	LOC159770	RAB34	ZC3HAV1
COX8A	GAPDH	lymphocyte activation antigen 4F2	RNF26	
Cpg132g6.rt1a	GNAS	microRNA pri-miR-21	RSBN1L	

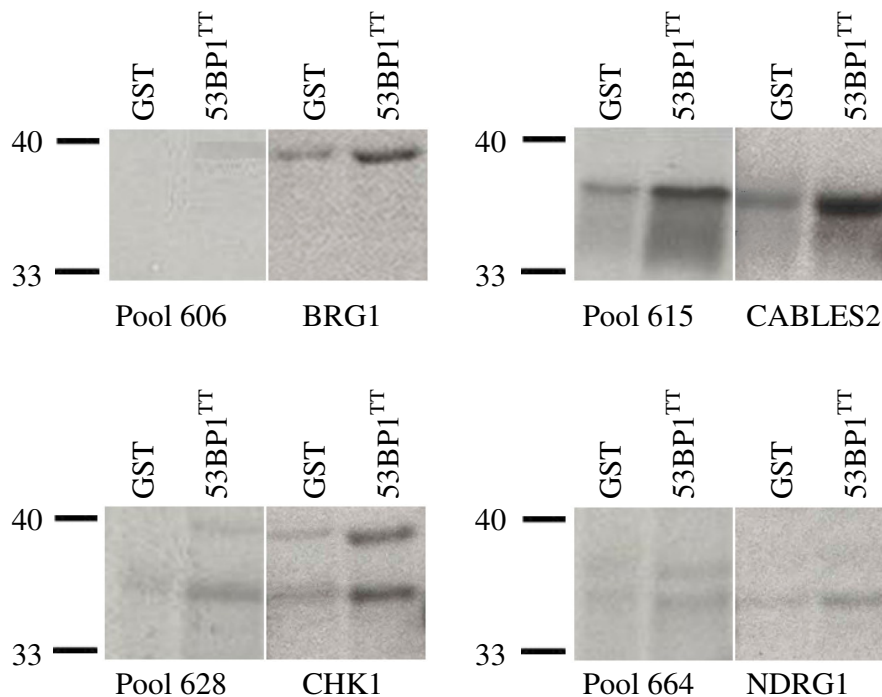


**Figure 8. Matching GST-pulldown results**

For each comparison group, the left panels represent the proteins from the target pools (refer to the arrows in Fig. 6) and the right panels represent the isolated proteins originated from the corresponding pools.

### Sequence alignment

Since the surrounding sequence is crucial for interaction between 53BP1<sup>TT</sup> and the methyl-lysine, my next objective was to identify the lysine residue and its surrounding sequence that could mediate 53BP1<sup>TT</sup> binding. Since the consensus sequence for 53BP1<sup>TT</sup> binding is not identified, I compared the BRG1 and CHK1 sequence to the known 53BP1<sup>TT</sup> domain binding sites in H4K20 and H3K79. The alignments were performed by the local sequence alignment function in CLC-

Sequence Viewer (CLC Bio). To optimize the alignment results, I separated the query sequences to multiple 100-residue segments and the consecutive segments contain 20-residue overlaps. A 21-peptide sequence centered on either H4K20 or H3K79 was used as a reference to the query sequences from the protein candidates.

The H4K20-CHK1 and H4K20-BRG1 alignment results show either matches or mismatches with similar polar surrounding regions. This implies the findings of potential 53BP1<sup>TT</sup> binding domains. In particular, the result indicated that BRG1 lysine 1375 (BRG1K1375) is the potential 53BP1<sup>TT</sup> binding residue (Fig. 9A). The alignment further demonstrated that both H4 and BRG1 contain a matching Arg-His-Arg-Lys (RHRK) sequence around H4K20 and BRG1K1375 respectively. Knowing that the H4 histidine H18 (H4H18) plays a critical role in the 53BP1<sup>TT</sup>-H4K20 interaction (Botuyan et al. 2006), the His-Arg-Lys (HRK) sequence near BRG1K1375 was hence considered crucial in mediating binding to 53BP1<sup>TT</sup>. I also identified a matching sequence Asp-Phe-Lys (DFK) from H3K79-CHK1 and H3K79-BRG1 sequence alignment (Fig. 9B). The results, in contrast to H4K20 alignments, displayed mismatches or long gaps around the corresponding DFK sequence.

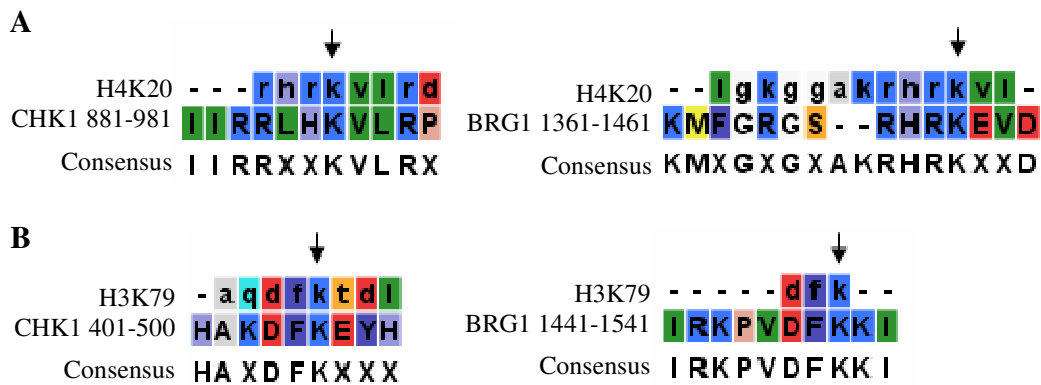


**Figure 9. Sequence alignment of CHK1 and BRG1 protein sequences with H3K79 or H4K20 as reference sequences**

The alignment results displayed were the best matches along the whole query sequences, CHK1 (left) and BRG1 (right). The consensus lane indicates match with corresponding residues. “X” denotes a mismatch and hyphen denotes gaps. A) Alignment using H4K20 as template. B) Alignment using H3K79 as template.

### **Endogenous BRG1 and CHK1 in HeLa cells interact with GST-53BP1<sup>TT</sup> domain**

Since the cDNA pools encode truncated proteins, my next objective was to determine the interactions between 53BP1<sup>TT</sup> domain and the full-length proteins. GST-pulldown assays on cell lysates were performed. HeLa cells were lysed and incubated with GST alone or 53BP<sup>TT</sup> domain, which covalently bound to glutathione-sepharose beads. The bound proteins were separated by SDS-PAGE and BRG1 and CHK1 were visualized by immunoblotting. I confirmed that endogenous BRG1 and CHK1 interact with GST-53BP<sup>TT</sup> domain. The H4K20me2 antibody was used as a positive control (Fig. 10A).

## **Effects of DSB on the binding affinity of 53BP1<sup>TT</sup> domain**

Since both 53BP1 and BRG1 are functionally involved in response to DSBs, I intended to further determine whether the 53BP1<sup>TT</sup> domain-BRG1 binding was associated to the DSB response. In this experiment, DNA damage was induced in HeLa cells by using etoposide phosphate, a topoisomerase II inhibitor. The cells were lysed in 1% Triton based lysis buffer. The cell lysates were subjected to GST-pulldown assay, SDS-PAGE and immunoblotting in sequence as described previously. Both CHK1 and BRG1 were visualized. The similar signal intensity in the pulldown results showed that DSBs did not influence the accessibility of CHK1 and BRG1 to the 53BP1<sup>TT</sup> domain (Fig. 10B). I proposed to further determine the effect of DSBs on BRG1 solubility since BRG1 becomes more resistant to detergent extraction after it localizes to the chromatin (Park et al. 2006). I induced DSBs using etoposide phosphate at a final concentration of 20 $\mu$ M on HeLa cells for 24 hours, and then lysed cells by using a Triton based lysis buffer. The insoluble fractions were subjected to acid extraction with 2N HCl. Western blot analysis was performed to compare the BRG1 abundance between the cell lysate fraction and the acid extraction fraction. Intriguingly, in response to DNA damage, BRG1 became vaguely detectible in Triton lysate and presented mainly in acid extracts (Fig. 10C). This suggests that DSBs promote the migration of BRG1 to chromatin.

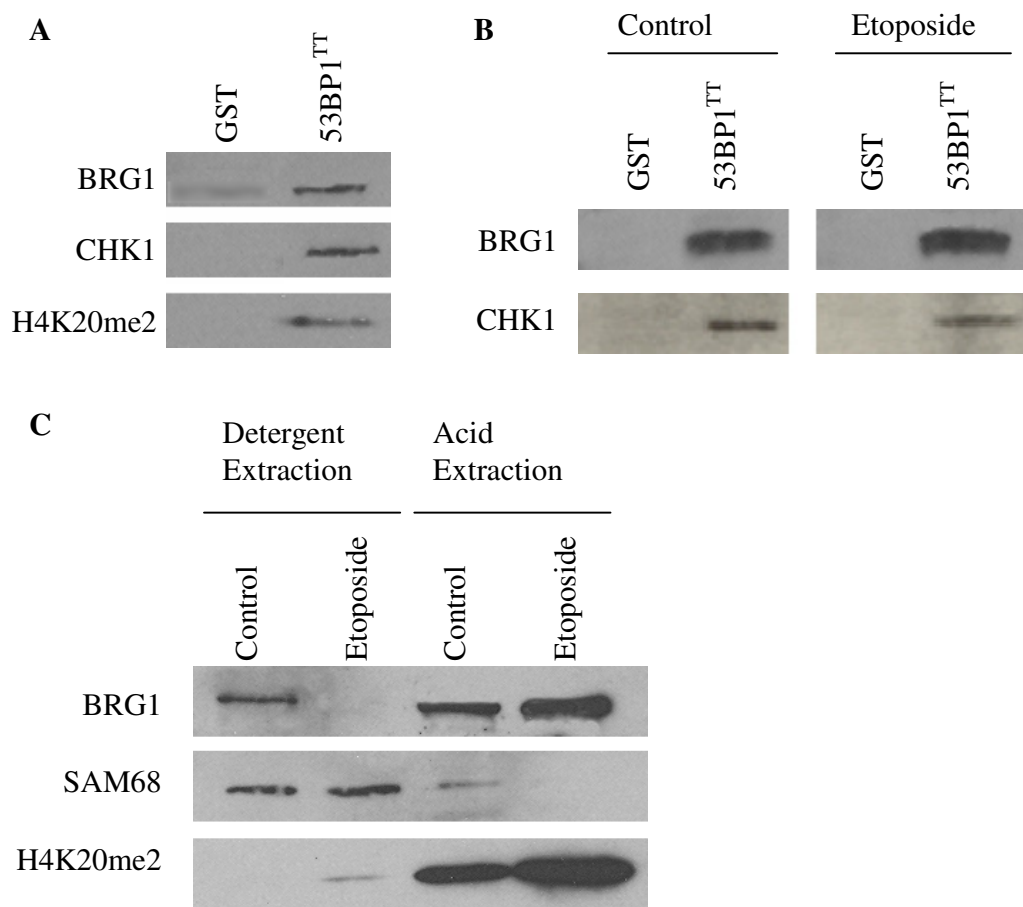


**Figure 10. GST-pulldown assays using total cell lysates**

Cells were lysed using Triton based lysis buffer. DSBs were induced by overnight treatment of 20 $\mu$ M etoposide phosphate. A) GST-pulldown assay using untreated cells, the H4K20me2 panel was used as control. B) GST-pulldown assay comparing cells with or without DSBs. C) Comparison of abundance of BRG1 in different cell fractions, with or without DSBs.

### **HRK motif in BRG1**

My results suggested a possible role of 53BP1-BRG1 interaction during DNA damage. Next, I intended to determine the 53BP1<sup>TT</sup> binding sites in BRG1. I

hypothesized that the BRG1 HRK motif is the potential binding site based on the sequence alignment analysis. I expressed the BRG1:1080-1395 fragment containing the HRK motif (1373-1375) and BRG1:1080-1360, with the deletion of the HRK motif, respectively using IVT system (Fig. 11A). GST-pulldown assays using radioactive-labeled IVT products revealed that 53BP1<sup>TT</sup> pulled down BRG1:1080-1395 but not BRG1:1080-1360 (Fig. 11B). The results suggest that the BRG1 region 1360-1395 is crucial for 53BP1<sup>TT</sup> binding. Based on the binding properties of 53BP1<sup>TT</sup>, I decided to further study the effect of dimethylation of BRG1K1375 (BRG1K1375me<sub>2</sub>) on 53BP1<sup>TT</sup> binding. Biotinylated peptides corresponding to the surroundings of the BRG1K1375 were synthesized with or without dimethyl-K1375. These peptides were used in ELISA to determine the role of BRG1K1375 methylation on 53BP1<sup>TT</sup> binding activity. ELISA on 53BP1<sup>TT</sup>-BRG1K1375me<sub>2</sub> show significantly strong binding affinity compared to the non-methylated counterpart or the unrelated control peptides (Fig. 11C). These results suggest that lysine methylation in the HRK motif significantly enhances 53BP1-BRG1 interaction.

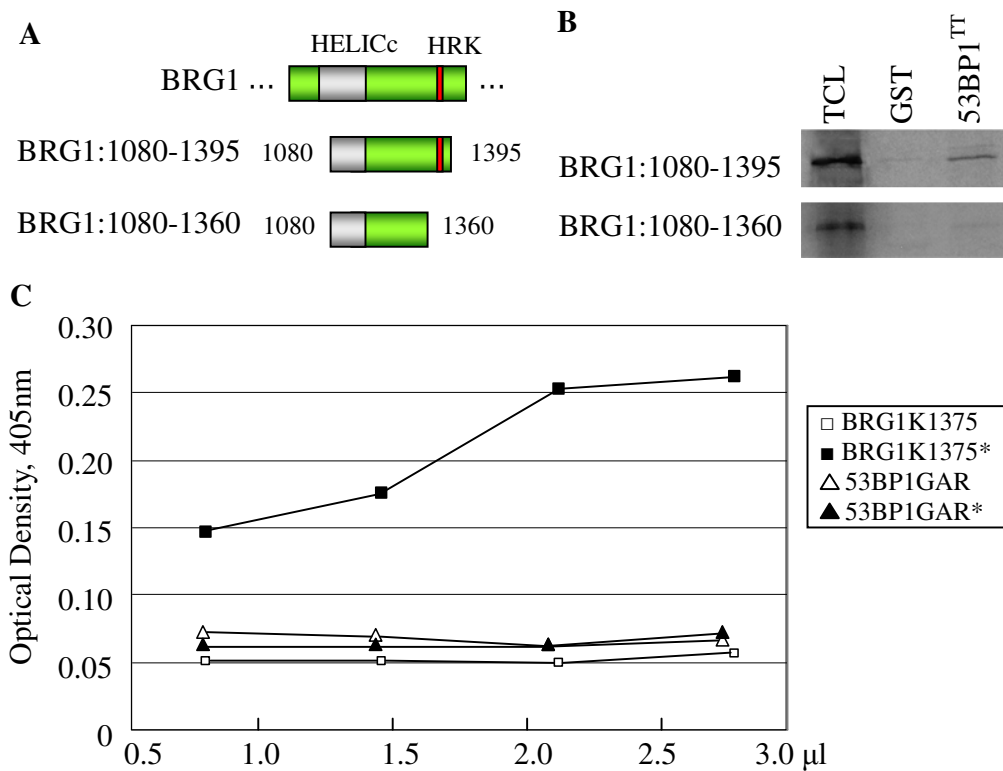


**Figure 11. The BRG1 HRK motif and its role in 53BP1<sup>TT</sup> binding**

The BRG1 HRK motif was identified by sequence alignment with peptide near H4K20. A) Schematic representation of truncated BRG1:1080-1395 and BRG1:1080-1360. The indicated HRK motif spans residues 1373-1375. B) GST-pulldown assay of BRG1:1080-1395 and BRG1:1080-1360 IVT products. C) ELISA analysis, peptides surround BRG1K1375 and 53BP1 GAR region, methylated (denoted by asterisk mark) and non-methylated, were used to determine the 53BP1<sup>TT</sup> binding target.

### ***In vivo* 53BP1-BRG1 interaction is associated to DNA damage**

I have shown that 53BP1<sup>TT</sup> binds to BRG1. My next objective was to determine the relationship between 53BP1 and BRG1 *in vivo*. HA-tagged 53BP1

(HA-53BP1) and V5-tagged BRG1 were co-expressed in HeLa cells and immunoprecipitated from cell lysate using anti-HA and anti-BRG1 antibodies respectively. Rabbit immunoglobulin G (IgG) was used as control. The immunoprecipitation samples were subjected to immunoblotting analysis with either anti-HA or anti-BRG1 antibodies. As shown in Fig. 12A and 12B, HA-53BP1 was co-immunoprecipitated by BRG1, and BRG1 was co-immunoprecipitated by HA-53BP1. We next examined whether the endogenous 53BP1-BRG1 interaction is DNA damage dependent. HeLa cells, treated with etoposide phosphate or left untreated, were lysed by Triton based lysis buffer. The cell lysates were subjected to brief sonication to shear the chromatin and increase the solubility of chromatin bound proteins. 53BP1 was observed to co-immunoprecipitate with BRG1 (Fig. 12C, Top), and vice versa (Fig. 12C, Bottom). Intriguingly, the co-immunoprecipitation was observed only in damage induced cells, suggesting that the 53BP1-BRG1 interaction is associated to DNA damage.

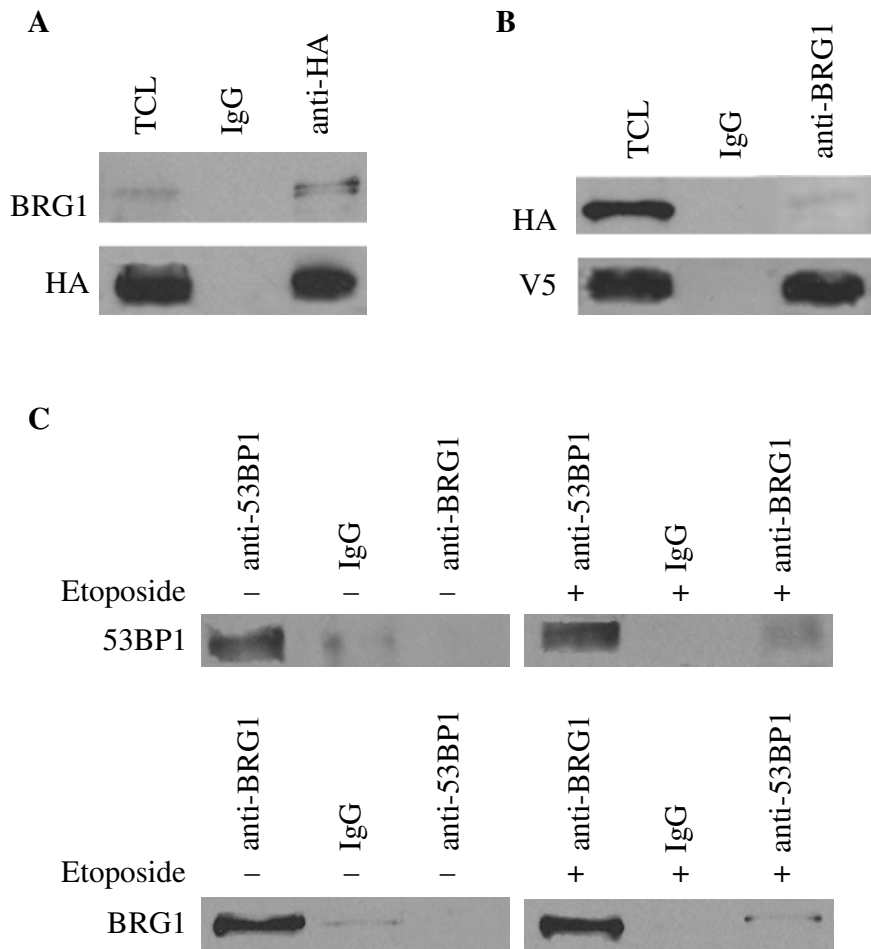


**Figure 12. *In vivo* co-immunoprecipitation of V5-BRG1 and HA-53BP1**

HeLa cells were co-transfected with V5-BRG1 and HA-53BP1. Cell lysates were subjected to immunoprecipitation as indicated and immunoblotted with anti-HA (A) and anti-BRG1 (B) antibodies. Total immunoprecipitated proteins were detected by anti-HA and anti-V5 antibodies. C) Co-immunoprecipitation *in vivo* in the presence or absence of etoposide phosphate.

### **BRG1 can be methylated *in vivo***

Since 53BP1<sup>TT</sup> bound to BRG1 in cell lysates and the binding is methyl-

lysine dependent, I extended the characterization of the methylation of BRG1 *in vivo*. To achieve this objective, metabolic labeling using radioactive [methyl-<sup>3</sup>H]-methionine was used *in vivo*. Src-associated in mitosis 68 kDa protein (SAM68) was used as a positive control. BRG1 and SAM68 were immunoprecipitated from the cell lysates using anti-BRG1 and anti-SAM68 antibodies respectively. The proteins were separated by SDS-PAGE and visualized by fluorography. The result revealed a faint, but definite methylation, suggesting that BRG1 is indeed methylated *in vivo* (Fig. 13).

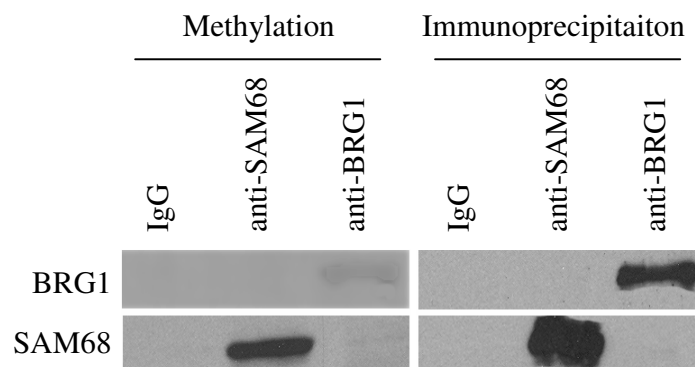


**Figure 13. *In vivo* methylation assay**

Radioactive [methyl-<sup>3</sup>H]-methionine was added as the methyl-donor to HeLa cell culture. Protein synthesis in HeLa cells were inhibited by the application of cycloheximide and chloramphenicol. Immunoprecipitation using anti-SAM68 and anti-BRG1 antibodies was applied to cell lysates to maintain the specificity of the proteins of interest.

### **BRG1K1375 methylation in response to DSBs**

I have observed that DNA damage enhances the 53BP1<sup>TT</sup> binding to BRG1 (Fig. 12C) and that the BRG1K1375me2 demonstrated high affinity to

53BP1<sup>TT</sup> (Fig. 11C). To examine whether BRG1K1375 is methylated *in vivo*, we generated anti-BRG1K1375me2 antibody. ELISA confirmed that this antibody was methyl-specific as it recognized the BRG1K1375me2 but not the unmethylated BRG1K1375 (Fig. 14A). Western analysis further determined that anti-BRG1K1375me2 recognized methylated BRG1 in undamaged HeLa cells (Fig. 14B), implying that BRG1K1375 methylation may be independent of DNA damage. Interestingly, stronger BRG1 methylation signal was observed from western blot analysis using DNA damaged HeLa cells which may suggest an alteration in BRG1K1375me2 accessibility (Fig. 14B). These findings show that BRG1 is methylated *in vivo* and that BRG1K1375me2 is an *in vivo* methyl mark.

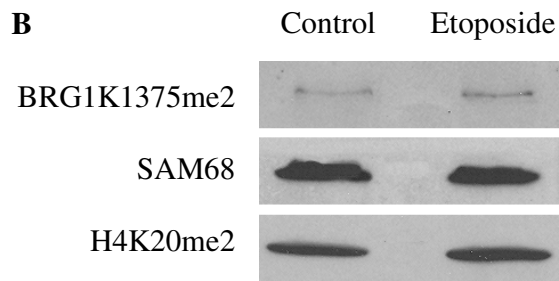
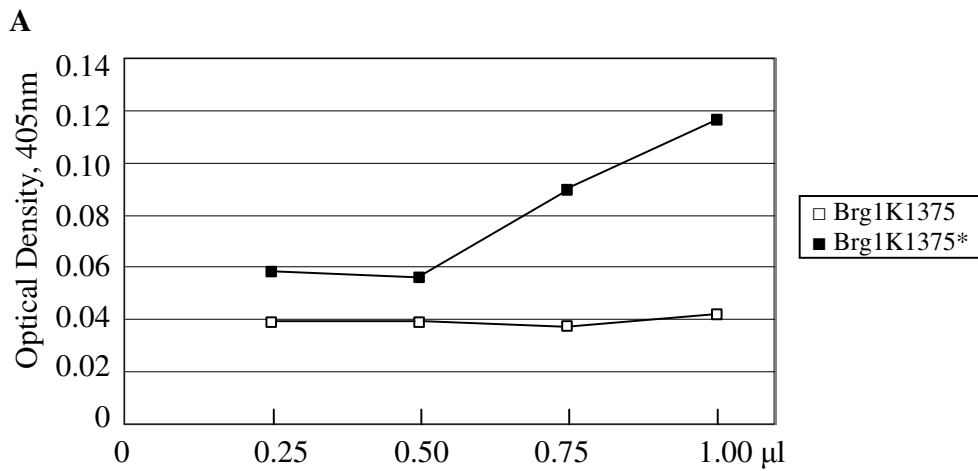


**Figure 14. Anti-BRG1K1375me2 detects BRG1 HRK\* motif**

A) ELISA confirms the binding specificity of anti-BRG1K1375me2 antibody. Peptides mapping surroundings of the HRK motif were tested. The asterisk mark denotes the dimethyl-lysine in the HRK motif. B) Western blot used anti-BRG1K1375me2 as primary antibody. Both SAM68 and H4K20me2 were used as the controls.

## Discussion

53BP1 plays a critical role in both DSB signaling and repair. Its functional importance in chromatin stability has been the focus of recent studies (Stucki et al. 2004; Boisvert et al. 2005). Furthermore, 53BP1 localizes to chromatin by recognizing dimethyl-lysine marks, H4K20 and H3K79 through the 53BP1<sup>TT</sup> domain (Xie et al. 2007). Hence, proteins that are recognized by 53BP1<sup>TT</sup> domain may potentially be methylated and associated with the DSB response. In this study, I identified BRG1 and CHK1 as two novel 53BP1<sup>TT</sup> domain targets.

I demonstrated the identification of 53BP1<sup>TT</sup> binding partners through proteomic screening of human cDNA library. 100 transformants were harvested from each target pool and were used for the proteomic screening. Alternatively, it is possible to increase the chance of finding a hit using recursive sib (sibling) selection procedure. Sibling pools can be generated by taking partial of the total amount of transformants. The sibling pools can be subsequently used for the next round of IVT expression selection (Fig. 15). Recursive application of sib selection could effectively narrow down the number of targets in large-scale proteomic screening. However, the screening procedure in this thesis has proven to be sufficient without sib selection.

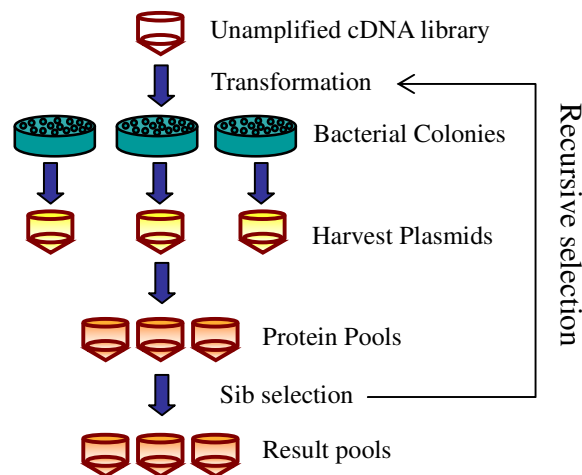


**Figure 15. Recursive sib selection flow chart**

Schematic presentation of recursive sib selection. The sib selection method varies depend on selection criteria.

Sequences (approximately 200 bps) obtained from Genome Quebec were sufficient for gene identification and for region mapping. In this thesis, the genes of interest were determined from sequence identification. Since the IVT system expresses genes by recognizing plasmid start codons, inserts that mapped to either open reading frames (ORFs) or the untranslated regions (UTRs) could be synthesized. Inserts that map to BRG1 ORF, CHK1 ORF, CABLES2 UTR, and NDRG1 UTR were resolved by mapping their sequences to their corresponding genes. The latter two UTR hits were not considered for the characterization since they do not encode functional proteins. Although BRG1 and CHK1 inserts mapped to the open reading frames, the identified sequences were insufficient to determine the whole inserts. The BRG1 insert was mapped from residue 463,

which corresponds to the helicases and associated with switching-defective protein 3, adaptor 2, nuclear receptor co-repressor, transcription factor (SANT) domain (HSA). HSA domain was found to bind nuclear actin-related proteins and has a role in regulating chromatin-remodeling ATPase (Szerlong et al. 2008). However, the functions of HSA was not well established. Since the 3' end of the BRG1 insert could not be determined, it is possible that the insert covers more than one functional domain in BRG1. The CHK1 insert was mapped inside the serine/threonine protein kinases catalytic domain - the only functional domain in CHK1. However, the length of the insert was not determined. To identify the potential binding sites, I performed sequence alignment on whole query sequences (BRG1 and CHK1) against the known 53BP1<sup>TT</sup> binding sites (K4K20 and H3K79). Both BRG1 and CHK1 contain potential 53BP1<sup>TT</sup> domain binding sites and their potential functional involvements in 53BP1 bindings were brought to attention.

CHK1 was proposed as one of the 53BP1 binding partners in this thesis. It is a checkpoint kinase which is the primary signal transducer linking activation of the ATM/ATR kinases to CDC25 homolog A (CDC25A) destruction in responses to IR (Jin et al. 2008). CHK1 is required for checkpoint mediated cell cycle arrest in response to DNA damage or the presence of unreplicated DNA (Zeng et al. 1999). CHK1 may also negatively regulate cell cycle progression during unperturbed cell cycles (Lam et al. 2004). Taken together with the functions of 53BP1, it is possible that CHK1 interacts with 53BP1 since both proteins

mediates ATM-associated DSB response pathways. Furthermore, this argument is strengthened by reports of interaction between CHK1 and yeast homologs of 53BP1, CRB2 and RAD9 (Mochida et al. 2004; Dang et al. 2005). In this thesis, I discovered the first evidence of the interaction between CHK1 and the mammalian 53BP1.

More interestingly, both sequence analysis and *in vivo* interactions revealed BRG1 as a 53BP1 binding partner. BRG1 is an ATP-dependent helicase, which is the core catalytic subunit of switch/sucrose nonfermentable (SWI/SNF) chromatin remodeling complex. It functions as a transcriptional coactivator cooperating with nuclear hormone receptors to potentiate transcriptional activation (Medina et al. 2008). BRG1 functions have been associated with cell growth control, apoptosis and senescence (Napolitano et al. 2007). BRG1 mutants were found in various tumor cell lines that have links between BRG1 and genomic stability (Wong et al. 2000). This is consistent with the enhanced expression of p53 target genes in the presence of both BRG1 and p53, but not with either BRG1 or p53 alone (Xu et al. 2007; Oh et al. 2008). Recent studies further suggested that BRG1 is recruited to DSB sites and associated to DSB repair (Park et al. 2006; Bao et al. 2007). Functionally, the SWI/SNF chromatin remodeling complex unwinds the tightly packed chromatin structure, renders the DSB sites accessible for repair (Altaf et al. 2007). In yeast, the inositol-requiring protein 80 (INO80) chromatin remodeling and the DNA damage pathway has been determined (Morrison et al. 2004). DSBs in mammalian cells may also

trigger similar ATP-dependent chromatin remodeling responses. Recently, the chromatin remodeling was shown to relate to carcinogenesis and its roles of cell cycle control was elaborated (Wang et al. 2007; Morettini et al. 2008). The discovery of BRG1 and 53BP1 interaction establishes a novel link in the context of chromatin remodeling and DNA damage responses.

My data show that both BRG1 and CHK1 bind to 53BP1<sup>TT</sup> domain *in vivo* in both HeLa and HEK293T cell lysates. Intriguingly, the 53BP1<sup>TT</sup>-BRG1 binding level was significantly lower when using HEK293T cell lysates. However, altered expression of BRG1 has been observed in some immortal cell lines (Napolitano et al. 2007; Medina et al. 2008) and this might, therefore, explain the low BRG1 expression in HEK293T cell line. The observed difference may due to the distinct origins between HeLa and HEK293 cell lines. However, the 53BP1<sup>TT</sup>-CHK1 binding level was relatively constant in both cell lines. Both BRG1 and CHK1 have been previously linked to DSB responses based on the role of 53BP1 in DNA damage. In response to DSBs, BRG1 migrates to chromatin and becomes more resistant to detergent extraction (Park et al. 2006). This implied low BRG1 solubility in DNA damaged cell lysate which makes it difficult to detect BRG1 associated interaction. We, therefore, lightly sonicated the cells and shear the chromatin and increase the BRG1 solubility. This technique was applied to endogenous co-IP and revealed that 53BP1-BRG1 interaction is dependent to DSB signals. The solubility of CHK1, on the other hand, was not affected by DNA damage.

It is known that 53BP1<sup>TT</sup> domain binds to H4K20me2 (Kim et al. 2006). Recent studies indicate that 53BP1<sup>TT</sup> domain also binds to tumor protein p53 lysine 370 (p53K370) in dimethylated state (p53K370me2) (Huang et al. 2007; Taverna et al. 2007). In this thesis, I demonstrated that BRG1 can be methylated *in vivo* and identified BRG1K1375me2 as a potential 53BP1<sup>TT</sup> domain binding ligand. These results demonstrated that the 53BP1<sup>TT</sup> domain binding is lysine dimethylation dependent. Therefore, transferases involved in BRG1K1375 methylation are the potential regulators of 53BP1-BRG1 interaction. Although the identification of these transferases was beyond the scope of my thesis, I, based on the sequence analysis, speculate that the methyltransferases Set8 and Suppressor of variegation 4-20 homolog 1/homolog 2 (Suv4-20h1/h2) which respectively mono- and di- methylate H4K20 (Yin et al. 2005; Yang et al. 2008) may also methylate the BRG1K1375. The jumonji domain containing 2A (JMJD2A), which remove methyl group from histone lysines H3K9, H3K27, and H4K20, was speculated to demethylate BRG1K1375me2 (Wang et al. 2007). However, identifying the transferases involved in BRG1 methylation and solidifying the functional importance of BRG1K1375 would require a BRG1 construct with a K1375 mutant.

In this thesis, I further revealed that the HRK motif, which presents in both H4 and BRG1, is required for efficient binding. In addition, the polarity surrounding HRK motif was positively charged and is a complement to the negatively charged 53BP1<sup>TT</sup> domain surface. Biochemical analysis further

revealed that histidine H4H18 was critical for 53BP1<sup>TT</sup> binding (Botuyan et al. 2006). The BRG1 HRK motif is conserved through mammalian species (Fig. 16). Cross species sequence analysis on BRG1 and its corresponding homologs, SNF2 and RSC complex subunit (STH1), revealed a conserved motif GRG(S/A)R(H/Q/E)RK (Fig. 16). I named it the 53BP1<sup>TT</sup> binding motif (53BP1<sup>TT</sup>BM). In addition, the conserved mammalian histidine in this motif varies across species according to higher order of organism classification (Fig. 16). This implies that the functional involvement of the interaction between 53BP1 and BRG1 may be of evolutionary significance. Moreover, there is a glycine-rich region located at the N-terminus of the 53BP1<sup>TT</sup>BM in both H4 and BRG1. This region usually indicates possible downstream loop structure and may potentially form the interface required for interacting with 53BP1. The BRG1 homolog, brahma (BRM), however, does not contain the 53BP1<sup>TT</sup>BM pattern and implies no 53BP1 association (Fig. 16).

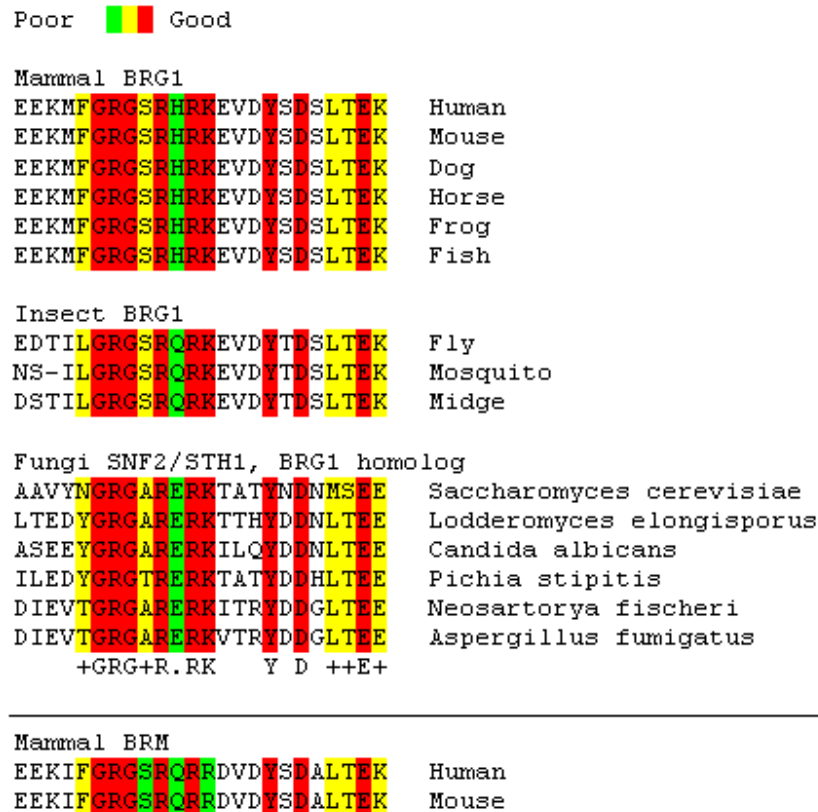


**Figure 16. Sequence alignment of 53BP1<sup>TT</sup> binding motif across species**

BRG1 and BRM sequences were obtained from the NCBI database. Species were briefly grouped by their taxonomic classification.

This thesis demonstrated that the *in vivo* 53BP1-BRG1 interaction is methylation dependent and is DNA damage associated. However, initiation of the interaction and its functional relevance were not elucidated. In response to DSBs, BRG1 might undergo a conformational change or a non-spontaneous BRG1K1375 dimethylation. I proposed that the 53BP1<sup>TT</sup>-BRG1 interaction was elevated through one of the modification model. In the conformation change

model, the BRG1K1375 mark is proposed to be dimethylated and inaccessible after protein synthesis. The DNA damage triggers BRG1 conformational change and exposes the BRG1K1375me<sub>2</sub> mark enabling 53BP1 binding. This recapitulates a previous suggestion that the histone methyl marks are exposed by DNA damage and subsequently recruits 53BP1 to the DSB site (Bekker-Jensen et al. 2005). In this thesis, the conformation change model is consistent with the absence of 53BP1-BRG1 interaction (Fig. 12C) while BRG1K1375me<sub>2</sub> was presented in the non-damaged cells (Fig. 14B). The exposed BRG1 53BP1<sup>TT</sup>BM, which resides in between BRG1 helicase domain and bromo domain, may behave like methylated histone tails and allow 53BP1 binding. In contrast, the non-spontaneous methylation model states that BRG1K1375 methylation was induced by DNA damage. It is also possible that DNA damage exposes the non-methylated BRG1K1375 mark, which is subsequently methylated. The dimethylated BRG1K1375 then promotes the 53BP1-BRG1 interaction. This model suggests that a DNA damage inducible BRG1K1375 methyltransferase may play a critical role in BRG1 methylation.

Since 53BP1<sup>TT</sup> domain contains single ligand binding site, I further proposed that its bindings to methyl-histone lysine marks and to the BRG1K1375me<sub>2</sub> mark are mutually exclusive. Based on the 53BP1 DSB surveillance function (Bekker-Jensen et al. 2005), I speculate that 53BP1 recruits BRG1, or possibly the BRG1-containing SWI/SNF chromatin remodeling complex, to the DNA damage site. DNA damage triggers both 53BP1 localization

to the DSB site by its tandem Tudor domain and the exposure of BRG1K1375me2 mark based on my thesis. The 53BP1 GAR motif then mediates DNA binding activity (Boisvert et al. 2005) and may disassociate the 53BP1<sup>TT</sup>-histone binding. The unbounded 53BP1<sup>TT</sup> domain subsequently recruits BRG1 and the associated chromatin remodeling complex, which then unwinds the chromatin structure surround the DSB site and opens access for other DNA repair associated proteins. The localization of BRG1 and 53BP1 can be visualized by fluorescence microscopy, and the knockdown of either protein can reveal the functional relevance of the interaction.

In summary, I have identified BRG1 and CHK1 as binding partners of 53BP1 through proteomic screening. I determined that the dimethylated K1375 within BRG1 is the 53BP1<sup>TT</sup> binding site. Furthermore, I demonstrated that BRG1-53BP1 interaction is associated to DSB responses *in vivo*. Although the regulatory mechanism of BRG1 methylation and the dynamic association and disassociation between BRG1 and 53BP1 in living cells remain to be studied, this study revealed a novel functional involvement of chromatin remodeling in response to DNA damage.

## References

- Adams, M. M., B. Wang, et al. (2005). "53BP1 oligomerization is independent of its methylation by PRMT1." Cell Cycle **4**(12): 1854-61.
- Altaf, M., N. Saksouk, et al. (2007). "Histone modifications in response to DNA damage." Mutat Res **618**(1-2): 81-90.
- Altschul, S. F., W. Gish, et al. (1990). "Basic local alignment search tool." J Mol Biol **215**(3): 403-10.
- Amikura, R., K. Hanyu, et al. (2001). "Tudor protein is essential for the localization of mitochondrial RNAs in polar granules of *Drosophila* embryos." Mech Dev **107**(1-2): 97-104.
- Anderson, L., C. Henderson, et al. (2001). "Phosphorylation and rapid relocalization of 53BP1 to nuclear foci upon DNA damage." Mol Cell Biol **21**(5): 1719-29.
- Aravind, L., D. R. Walker, et al. (1999). "Conserved domains in DNA repair proteins and evolution of repair systems." Nucleic Acids Res **27**(5): 1223-42.
- Bakkenist, C. J. and M. B. Kastan (2003). "DNA damage activates ATM through intermolecular autophosphorylation and dimer dissociation." Nature **421**(6922): 499-506.
- Bao, Y. and X. Shen (2007). "Chromatin remodeling in DNA double-strand break repair." Curr Opin Genet Dev **17**(2): 126-31.
- Bekker-Jensen, S., C. Lukas, et al. (2005). "Dynamic assembly and sustained retention of 53BP1 at the sites of DNA damage are controlled by Mdc1/NFBD1." J Cell Biol **170**(2): 201-11.
- Boisvert, F. M., A. Rhie, et al. (2005). "The GAR motif of 53BP1 is arginine methylated by PRMT1 and is necessary for 53BP1 DNA binding activity." Cell Cycle **4**(12): 1834-41.
- Botuyan, M. V., J. Lee, et al. (2006). "Structural basis for the methylation state-specific recognition of histone H4-K20 by 53BP1 and Crb2 in DNA repair." Cell **127**(7): 1361-73.
- Cadet, J., T. Douki, et al. (2003). "Oxidative damage to DNA: formation, measurement and biochemical features." Mutat Res **531**(1-2): 5-23.
- Celeste, A., O. Fernandez-Capetillo, et al. (2003). "Histone H2AX phosphorylation is dispensable for the initial recognition of DNA breaks." Nat Cell Biol **5**(7): 675-9.

- Charier, G., J. Couprie, et al. (2004). "The Tudor tandem of 53BP1: a new structural motif involved in DNA and RG-rich peptide binding." *Structure* **12**(9): 1551-62.
- Chen, P., M. Gatei, et al. (1999). "Chk1 complements the G2/M checkpoint defect and radiosensitivity of ataxia-telangiectasia cells." *Oncogene* **18**(1): 249-56.
- Cheng, D., J. Cote, et al. (2007). "The arginine methyltransferase CARM1 regulates the coupling of transcription and mRNA processing." *Mol Cell* **25**(1): 71-83.
- Costanzo, V., D. Shechter, et al. (2003). "An ATR- and Cdc7-dependent DNA damage checkpoint that inhibits initiation of DNA replication." *Mol Cell* **11**(1): 203-13.
- Cote, J. and S. Richard (2005). "Tudor domains bind symmetrical dimethylated arginines." *J Biol Chem* **280**(31): 28476-83.
- d'Adda di Fagagna, F., P. M. Reaper, et al. (2003). "A DNA damage checkpoint response in telomere-initiated senescence." *Nature* **426**(6963): 194-8.
- Dang, T., S. Bao, et al. (2005). "Human Rad9 is required for the activation of S-phase checkpoint and the maintenance of chromosomal stability." *Genes Cells* **10**(4): 287-95.
- Derbyshire, D. J., B. P. Basu, et al. (2002). "Crystal structure of human 53BP1 BRCT domains bound to p53 tumour suppressor." *EMBO J* **21**(14): 3863-72.
- DiTullio, R. A., Jr., T. A. Mochan, et al. (2002). "53BP1 functions in an ATM-dependent checkpoint pathway that is constitutively activated in human cancer." *Nat Cell Biol* **4**(12): 998-1002.
- Falck, J., J. Coates, et al. (2005). "Conserved modes of recruitment of ATM, ATR and DNA-PKcs to sites of DNA damage." *Nature* **434**(7033): 605-11.
- Fry, R. C., T. J. Begley, et al. (2005). "Genome-wide responses to DNA-damaging agents." *Annu Rev Microbiol* **59**: 357-77.
- Goodarzi, A. A., A. T. Noon, et al. (2008). "ATM signaling facilitates repair of DNA double-strand breaks associated with heterochromatin." *Mol Cell* **31**(2): 167-77.
- Guccione, E., C. Bassi, et al. (2007). "Methylation of histone H3R2 by PRMT6 and H3K4 by an MLL complex are mutually exclusive." *Nature* **449**(7164): 933-7.
- Guo, J. Y., A. Yamada, et al. (2008). "Aven-dependent activation of ATM following DNA damage." *Curr Biol* **18**(13): 933-42.

- Hanawalt, P. C. and G. Spivak (2008). "Transcription-coupled DNA repair: two decades of progress and surprises." Nat Rev Mol Cell Biol **9**(12): 958-70.
- Harris, A. L. (1990). "Mutant p53--the commonest genetic abnormality in human cancer?" J Pathol **162**(1): 5-6.
- Hendricks, K. B., F. Shanahan, et al. (2004). "Role for BRG1 in cell cycle control and tumor suppression." Mol Cell Biol **24**(1): 362-76.
- Henning, W. and H. W. Sturzbecher (2003). "Homologous recombination and cell cycle checkpoints: Rad51 in tumour progression and therapy resistance." Toxicology **193**(1-2): 91-109.
- Huang, J., R. Sengupta, et al. (2007). "p53 is regulated by the lysine demethylase LSD1." Nature **449**(7158): 105-8.
- Huang, Y., J. Fang, et al. (2006). "Recognition of histone H3 lysine-4 methylation by the double tudor domain of JMJD2A." Science **312**(5774): 748-51.
- Huyen, Y., O. Zgheib, et al. (2004). "Methylated lysine 79 of histone H3 targets 53BP1 to DNA double-strand breaks." Nature **432**(7015): 406-11.
- Ishikawa, K., H. Ishii, et al. (2006). "DNA damage-dependent cell cycle checkpoints and genomic stability." DNA Cell Biol **25**(7): 406-11.
- Iwabuchi, K., P. L. Bartel, et al. (1994). "Two cellular proteins that bind to wild-type but not mutant p53." Proc Natl Acad Sci U S A **91**(13): 6098-102.
- Iwabuchi, K., B. P. Basu, et al. (2003). "Potential role for 53BP1 in DNA end-joining repair through direct interaction with DNA." J Biol Chem **278**(38): 36487-95.
- Iwabuchi, K., B. Li, et al. (1998). "Stimulation of p53-mediated transcriptional activation by the p53-binding proteins, 53BP1 and 53BP2." J Biol Chem **273**(40): 26061-8.
- Jazayeri, A., A. Balestrini, et al. (2008). "Mre11-Rad50-Nbs1-dependent processing of DNA breaks generates oligonucleotides that stimulate ATM activity." EMBO J **27**(14): 1953-62.
- Jin, J., X. L. Ang, et al. (2008). "Differential roles for checkpoint kinases in DNA damage-dependent degradation of the Cdc25A protein phosphatase." J Biol Chem **283**(28): 19322-8.
- Jiricny, J. (1998). "Replication errors: challenging the genome." EMBO J **17**(22): 6427-36.
- Joo, W. S., P. D. Jeffrey, et al. (2002). "Structure of the 53BP1 BRCT region

- bound to p53 and its comparison to the Brca1 BRCT structure." Genes Dev **16**(5): 583-93.
- Jowsey, P., N. A. Morrice, et al. (2007). "Characterisation of the sites of DNA damage-induced 53BP1 phosphorylation catalysed by ATM and ATR." DNA Repair (Amst) **6**(10): 1536-44.
- Jullien, D., P. Vagnarelli, et al. (2002). "Kinetochore localisation of the DNA damage response component 53BP1 during mitosis." J Cell Sci **115**(Pt 1): 71-9.
- Khanna, K. K. and S. P. Jackson (2001). "DNA double-strand breaks: signaling, repair and the cancer connection." Nat Genet **27**(3): 247-54.
- Kim, J., J. Daniel, et al. (2006). "Tudor, MBT and chromo domains gauge the degree of lysine methylation." EMBO Rep **7**(4): 397-403.
- Kobayashi, J., K. Iwabuchi, et al. (2008). "Current topics in DNA double-strand break repair." J Radiat Res (Tokyo) **49**(2): 93-103.
- Koike, M., J. Sugawara, et al. (2005). "p53 phosphorylation in mouse skin and in vitro human skin model by high-dose-radiation exposure." J Radiat Res (Tokyo) **46**(4): 461-8.
- Kuhne, C., M. L. Tjornhammar, et al. (2003). "Repair of a minimal DNA double-strand break by NHEJ requires DNA-PKcs and is controlled by the ATM/ATR checkpoint." Nucleic Acids Res **31**(24): 7227-37.
- Kurz, E. U. and S. P. Lees-Miller (2004). "DNA damage-induced activation of ATM and ATM-dependent signaling pathways." DNA Repair (Amst) **3**(8-9): 889-900.
- Lam, M. H. and J. M. Rosen (2004). "Chk1 versus Cdc25: chking one's levels of cellular proliferation." Cell Cycle **3**(11): 1355-7.
- Lee, J., J. R. Thompson, et al. (2008). "Distinct binding modes specify the recognition of methylated histones H3K4 and H4K20 by JMJD2A-tudor." Nat Struct Mol Biol **15**(1): 109-11.
- Lieber, M. R., K. Yu, et al. (2006). "Roles of nonhomologous DNA end joining, V(D)J recombination, and class switch recombination in chromosomal translocations." DNA Repair (Amst) **5**(9-10): 1234-45.
- Liu, Y. and S. C. West (2004). "Happy Hollidays: 40th anniversary of the Holliday junction." Nat Rev Mol Cell Biol **5**(11): 937-44.
- Luger, K., A. W. Mader, et al. (1997). "Crystal structure of the nucleosome core particle at 2.8 Å resolution." Nature **389**(6648): 251-60.

- Manis, J. P., J. C. Morales, et al. (2004). "53BP1 links DNA damage-response pathways to immunoglobulin heavy chain class-switch recombination." Nat Immunol **5**(5): 481-7.
- Marignani, P. A., F. Kanai, et al. (2001). "LKB1 associates with Brg1 and is necessary for Brg1-induced growth arrest." J Biol Chem **276**(35): 32415-8.
- Matsuoka, S., B. A. Ballif, et al. (2007). "ATM and ATR substrate analysis reveals extensive protein networks responsive to DNA damage." Science **316**(5828): 1160-6.
- Maurer-Stroh, S., N. J. Dickens, et al. (2003). "The Tudor domain 'Royal Family': Tudor, plant Agenet, Chromo, PWWP and MBT domains." Trends Biochem Sci **28**(2): 69-74.
- Medina, P. P. and M. S. Cespedes (2008). "Involvement of the chromatin-remodeling factor BRG1/SMARCA4 in human cancer." Epigenetics **3**(2): 64-8.
- Medina, P. P., O. A. Romero, et al. (2008). "Frequent BRG1/SMARCA4-inactivating mutations in human lung cancer cell lines." Hum Mutat **29**(5): 617-22.
- Minter-Dykhouse, K., I. Ward, et al. (2008). "Distinct versus overlapping functions of MDC1 and 53BP1 in DNA damage response and tumorigenesis." J Cell Biol **181**(5): 727-35.
- Mochan, T. A., M. Venere, et al. (2004). "53BP1, an activator of ATM in response to DNA damage." DNA Repair (Amst) **3**(8-9): 945-52.
- Mochida, S., F. Esashi, et al. (2004). "Regulation of checkpoint kinases through dynamic interaction with Crb2." EMBO J **23**(2): 418-28.
- Morettini, S., V. Podhraski, et al. (2008). "ATP-dependent chromatin remodeling enzymes and their various roles in cell cycle control." Front Biosci **13**: 5522-32.
- Morrison, A. J., J. Highland, et al. (2004). "INO80 and gamma-H2AX interaction links ATP-dependent chromatin remodeling to DNA damage repair." Cell **119**(6): 767-75.
- Napolitano, M. A., M. Cipollaro, et al. (2007). "Brg1 chromatin remodeling factor is involved in cell growth arrest, apoptosis and senescence of rat mesenchymal stem cells." J Cell Sci **120**(Pt 16): 2904-11.
- Neels, J. F., J. Gong, et al. (2007). "Quantitative correlation of drug bioactivation and deoxyadenosine alkylation by acylfulvene." Chem Res Toxicol **20**(10): 1513-9.
- O'Driscoll, M. and P. A. Jeggo (2006). "The role of double-strand break repair -

- insights from human genetics." Nat Rev Genet **7**(1): 45-54.
- Oh, J., D. H. Sohn, et al. (2008). "BAF60a interacts with p53 to recruit the SWI/SNF complex." J Biol Chem **283**(18): 11924-34.
- Oren, M. (2003). "Decision making by p53: life, death and cancer." Cell Death Differ **10**(4): 431-42.
- Park, J. H., E. J. Park, et al. (2006). "Mammalian SWI/SNF complexes facilitate DNA double-strand break repair by promoting gamma-H2AX induction." EMBO J **25**(17): 3986-97.
- Ponting, C. P. (1997). "Tudor domains in proteins that interact with RNA." Trends Biochem Sci **22**(2): 51-2.
- Rappold, I., K. Iwabuchi, et al. (2001). "Tumor suppressor p53 binding protein 1 (53BP1) is involved in DNA damage-signaling pathways." J Cell Biol **153**(3): 613-20.
- Rodriguez, R. and M. Meuth (2006). "Chk1 and p21 cooperate to prevent apoptosis during DNA replication fork stress." Mol Biol Cell **17**(1): 402-12.
- Saintigny, Y., F. Delacote, et al. (2007). "XRCC4 in G1 suppresses homologous recombination in S/G2, in G1 checkpoint-defective cells." Oncogene **26**(19): 2769-80.
- Sanders, S. L., M. Portoso, et al. (2004). "Methylation of histone H4 lysine 20 controls recruitment of Crb2 to sites of DNA damage." Cell **119**(5): 603-14.
- Schultz, L. B., N. H. Chehab, et al. (2000). "p53 binding protein 1 (53BP1) is an early participant in the cellular response to DNA double-strand breaks." J Cell Biol **151**(7): 1381-90.
- Selenko, P., R. Sprangers, et al. (2001). "SMN tudor domain structure and its interaction with the Sm proteins." Nat Struct Biol **8**(1): 27-31.
- Shi, Y. and J. R. Whetstine (2007). "Dynamic regulation of histone lysine methylation by demethylases." Mol Cell **25**(1): 1-14.
- Shimada, M. and M. Nakanishi (2006). "DNA damage checkpoints and cancer." J Mol Histol **37**(5-7): 253-60.
- Sonoda, E., G. Y. Zhao, et al. (2007). "Collaborative roles of gammaH2AX and the Rad51 paralog Xrcc3 in homologous recombinational repair." DNA Repair (Amst) **6**(3): 280-92.
- Soulas-Sprauel, P., P. Rivera-Munoz, et al. (2007). "V(D)J and immunoglobulin class switch recombinations: a paradigm to study the regulation of DNA end-

- joining." Oncogene **26**(56): 7780-91.
- Sprangers, R., M. R. Groves, et al. (2003). "High-resolution X-ray and NMR structures of the SMN Tudor domain: conformational variation in the binding site for symmetrically dimethylated arginine residues." J Mol Biol **327**(2): 507-20.
- Stewart, G. S., T. Stankovic, et al. (2007). "RIDDLE immunodeficiency syndrome is linked to defects in 53BP1-mediated DNA damage signaling." Proc Natl Acad Sci U S A **104**(43): 16910-5.
- Stiff, T., S. A. Walker, et al. (2006). "ATR-dependent phosphorylation and activation of ATM in response to UV treatment or replication fork stalling." EMBO J **25**(24): 5775-82.
- Stucki, M. and S. P. Jackson (2004). "Tudor domains track down DNA breaks." Nat Cell Biol **6**(12): 1150-2.
- Szerlong, H., K. Hinata, et al. (2008). "The HSA domain binds nuclear actin-related proteins to regulate chromatin-remodeling ATPases." Nat Struct Mol Biol **15**(5): 469-76.
- Talbot, K., I. Miguel-Aliaga, et al. (1998). "Characterization of a gene encoding survival motor neuron (SMN)-related protein, a constituent of the spliceosome complex." Hum Mol Genet **7**(13): 2149-56.
- Taverna, S. D., H. Li, et al. (2007). "How chromatin-binding modules interpret histone modifications: lessons from professional pocket pickers." Nat Struct Mol Biol **14**(11): 1025-40.
- Thorslund, T. and S. C. West (2007). "BRCA2: a universal recombinase regulator." Oncogene **26**(56): 7720-30.
- Trotter, K. W., H. Y. Fan, et al. (2008). "The HSA domain of BRG1 mediates critical interactions required for glucocorticoid receptor-dependent transcriptional activation in vivo." Mol Cell Biol **28**(4): 1413-26.
- Unger, T., M. M. Nau, et al. (1992). "p53: a transdominant regulator of transcription whose function is ablated by mutations occurring in human cancer." EMBO J **11**(4): 1383-90.
- Valerie, K. and L. F. Povirk (2003). "Regulation and mechanisms of mammalian double-strand break repair." Oncogene **22**(37): 5792-812.
- van Attikum, H. and S. M. Gasser (2005). "The histone code at DNA breaks: a guide to repair?" Nat Rev Mol Cell Biol **6**(10): 757-65.
- Vidanes, G. M., C. Y. Bonilla, et al. (2005). "Complicated tails: histone

- modifications and the DNA damage response." Cell **121**(7): 973-6.
- Vink, A. A. and L. Roza (2001). "Biological consequences of cyclobutane pyrimidine dimers." J Photochem Photobiol B **65**(2-3): 101-4.
- Wang, B., S. Matsuoka, et al. (2002). "53BP1, a mediator of the DNA damage checkpoint." Science **298**(5597): 1435-8.
- Wang, G. G., C. D. Allis, et al. (2007). "Chromatin remodeling and cancer, Part I: Covalent histone modifications." Trends Mol Med **13**(9): 363-72.
- Wang, G. G., C. D. Allis, et al. (2007). "Chromatin remodeling and cancer, Part II: ATP-dependent chromatin remodeling." Trends Mol Med **13**(9): 373-80.
- Ward, I. M., K. Minn, et al. (2003). "Accumulation of checkpoint protein 53BP1 at DNA breaks involves its binding to phosphorylated histone H2AX." J Biol Chem **278**(22): 19579-82.
- Wong, A. K., F. Shanahan, et al. (2000). "BRG1, a component of the SWI-SNF complex, is mutated in multiple human tumor cell lines." Cancer Res **60**(21): 6171-7.
- Wu, R. S. and W. M. Bonner (1981). "Separation of basal histone synthesis from S-phase histone synthesis in dividing cells." Cell **27**(2 Pt 1): 321-30.
- Xia, Z., J. C. Morales, et al. (2001). "Negative cell cycle regulation and DNA damage-inducible phosphorylation of the BRCT protein 53BP1." J Biol Chem **276**(4): 2708-18.
- Xie, A., A. Hartlerode, et al. (2007). "Distinct roles of chromatin-associated proteins MDC1 and 53BP1 in mammalian double-strand break repair." Mol Cell **28**(6): 1045-57.
- Xu, Y., J. Zhang, et al. (2007). "The activity of p53 is differentially regulated by Brm- and Brg1-containing SWI/SNF chromatin remodeling complexes." J Biol Chem **282**(52): 37429-35.
- Yang, H., J. J. Pesavento, et al. (2008). "Preferential dimethylation of histone H4 lysine 20 by Suv4-20." J Biol Chem **283**(18): 12085-92.
- Yin, Y., C. Liu, et al. (2005). "SET8 recognizes the sequence RHRK20VLRDN within the N terminus of histone H4 and mono-methylates lysine 20." J Biol Chem **280**(34): 30025-31.
- Zeng, Y. and H. Piwnica-Worms (1999). "DNA damage and replication checkpoints in fission yeast require nuclear exclusion of the Cdc25 phosphatase via 14-3-3 binding." Mol Cell Biol **19**(11): 7410-9.

## **Appendix**

The appendix contains the following item:

- Permission to the student for the use of biohazard materials